Complexin synchronizes primed vesicle exocytosis and regulates fusion pore dynamics

Madhurima Dhara,[1] Antonio Yarzagaray,[1] Yvonne Schwarz,[1] Soumyajit Dutta,[1] Chad Grabner,[1] Paanteha K. Moghadam,[1] Anneka Bost,[1] Claudia Schirra,[1] Jens Rettig,[1] Kerstin Reim,[2] Nils Brose,[2] Ralf Mohrmann,[1] and Dieter Bruns[1,3]

[1]Institute for Physiology, University of Saarland, 66424 Homburg/Saar, Germany
[2]Department of Molecular Neurobiology, Max-Planck Institute of Experimental Medicine, 37075 Göttingen, Germany

ComplexinII (CpxII) and SynaptotagminI (SytI) have been implicated in regulating the function of SNARE proteins in exocytosis, but their precise mode of action and potential interplay have remained unknown. In this paper, we show that CpxII increases Ca^{2+}-triggered vesicle exocytosis and accelerates its secretory rates, providing two independent, but synergistic, functions to enhance synchronous secretion. Specifically, we demonstrate that the C-terminal domain of CpxII increases the pool of primed vesicles by hindering premature exocytosis at submicromolar Ca^{2+} concentrations, whereas the N-terminal domain shortens the secretory delay and accelerates the kinetics of Ca^{2+}-triggered exocytosis by increasing the Ca^{2+} affinity of synchronous secretion. With its C terminus, CpxII attenuates fluctuations of the early fusion pore and slows its expansion but is functionally antagonized by SytI, enabling rapid transmitter discharge from single vesicles. Thus, our results illustrate how key features of CpxII, SytI, and their interplay transform the constitutively active SNARE-mediated fusion mechanism into a highly synchronized, Ca^{2+}-triggered release apparatus.

Introduction

Temporal precision and speed are crucial determinants of Ca^{2+}-regulated neurotransmitter release. To meet this task, secretory cells establish a pool of primed vesicles, which are ready to fuse in response to the triggering Ca^{2+} stimulus. Membrane-bridging interactions of neuronal SNARE proteins, i.e., the vesicular synaptobrevinII (SybII) and the two plasma membrane proteins SyntaxinI and SNAP-25, provide the molecular force, which drives vesicles into membrane merger (Weber et al., 1998; Nickel et al., 1999; Sørensen et al., 2006; Kesavan et al., 2007). Because SNARE proteins can assemble spontaneously, fast Ca^{2+}-triggered fusion requires regulating proteins, such as complexin (Cpx; McMahon et al., 1995; Chen et al., 2002), which potentially prevents premature completion of SNARE zippering (Giraudo et al., 2006), and SytI (Geppert et al., 1994), which is generally held to be the Ca^{2+} sensor of the release machinery (Chapman, 2008).

Cpx is a small cytosolic α-helical protein that binds to assembled SNARE complexes with high affinity and has multiple domains with controversially discussed functions (Brose, 2008). The N terminus of Cpx exhibits a stimulatory effect on evoked release in murine neurons (Xue et al., 2007; Maximov et al., 2009) but has no effect at the neuromuscular junction (NMJ) of *Caenorhabditis elegans* (Hobson et al., 2011; Martin et al., 2011). The accessory α helix, instead, exerts an inhibitory action in in vivo studies (Xue et al., 2007; Maximov et al., 2009; Yang et al., 2010), which may arise from interfering with the SybII binding to the Syntaxin–SNAP-25 heterodimer, a scenario that could prevent zippering of partially assembled SNARE complexes before the Ca^{2+} trigger (Giraudo et al., 2009; Krishnakumar et al., 2011; Kümmel et al., 2011). The central α helix of Cpx binds to the groove between the helices of SyntaxinI and SybII within the SNARE complex (Bracher et al., 2002;

M. Dhara and A. Yarzagaray contributed equally to this paper.

Correspondence to Dieter Bruns: dieter.bruns@uniklinik-saarland.de

Abbreviations used in this paper: ANOVA, analysis of variance; ChrgA, chromogranin A; CM, membrane capacitance; Cpx, complexin; dko, double ko; EB, exocytotic burst; ko, knockout; M_{Dis}, median distance; NMJ, neuromuscular junction; NP, nitrophenyl; rms, root–mean–square; RRP, readily releasable pool; SR, sustained rate; SRP, slowly releasable pool; SybII, synaptobrevinII; Syt, synaptotagmin; wt, wild type.

The Rockefeller University Press $30.00
J. Cell Biol. Vol. 204 No. 7 1123–1140
www.jcb.org/cgi/doi/10.1083/jcb.201311085

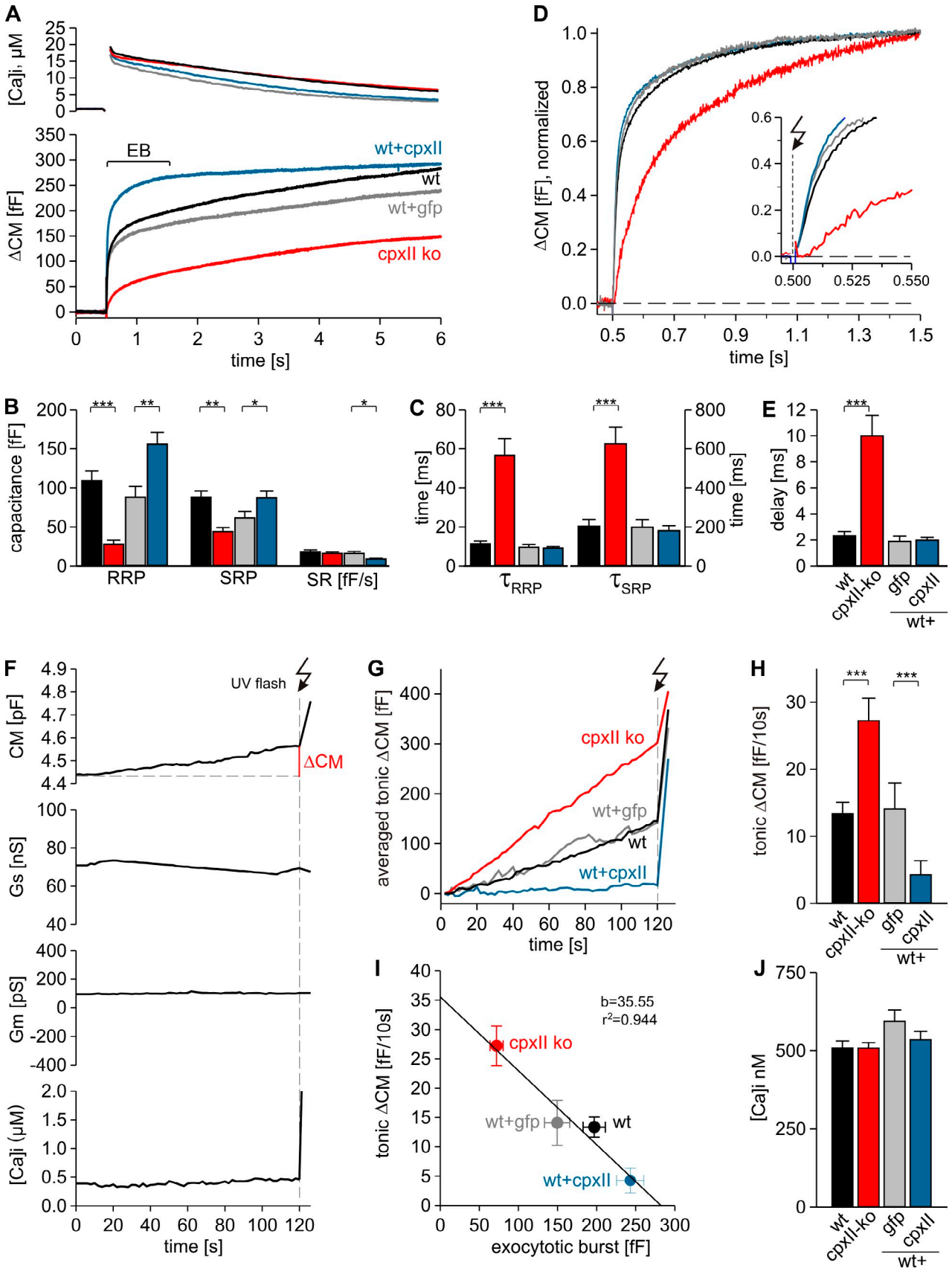

Figure 1. **CpxII controls magnitude and time course of synchronous exocytosis.** (A) Mean flash-induced $[Ca^{2+}]i$ levels (top) and corresponding CM responses (bottom) of wt (n = 26), CpxII ko (n = 33), and wt cells expressing either GFP (wt + gfp, n = 16) or CpxII (wt + CpxII, n = 23). Flash is at t = 0.5 s. (B) RRP and SRP size are reduced in the absence and increased with overexpression of CpxII. (C) CpxII loss slows the time constants of RRP and SRP

Chen et al., 2002), whereas the C-terminal region of Cpx comprising almost half of the protein binds to synaptotagmin (Syt; Tokumaru et al., 2008) or to phospholipids (Malsam et al., 2009; Seiler et al., 2009) and has been suggested either to be functionally inert (Xue et al., 2007) or to clamp spontaneous fusion (Cho et al., 2010; Martin et al., 2011; Kaeser-Woo et al., 2012). In particular, knockout (ko) and knockdown perturbations of Cpx in mice elicited controversies about its role in exocytosis. Genetic ablation of all Cpx isoforms expressed in the brain reduces both spontaneous and triggered release in hippocampal neurons and lowers the Ca^{2+} affinity of evoked secretion (Xue et al., 2007, 2010). In contrast, knockdown of Cpx by RNA interference in mass-cultured cortical neurons increases spontaneous and decreases evoked release, which exhibits a higher calcium affinity of secretion (Maximov et al., 2009; Yang et al., 2010; Cao et al., 2013). Although loss of evoked vesicle exocytosis is a common feature of Cpx mutants in all organisms studied (Reim et al., 2001; Giraudo et al., 2006, 2008; Schaub et al., 2006; Tang et al., 2006; Huntwork and Littleton, 2007; Xue et al., 2007, 2009, 2010; Cai et al., 2008; Yoon et al., 2008; Jorquera et al., 2012; Lin et al., 2013), the molecular mechanisms underlying facilitation as well as inhibition of release by Cpx remained controversial. Even more unclear is when and how the putative fusion clamp by Cpx is released in the process of Ca^{2+}-triggered exocytosis.

Given these open questions, we set out to delineate Cpx action in the vesicle release process and clarify to what extent its function is regulated by SytI. We show at submicromolar [Ca]i, the C-terminal domain of CpxII prevents premature vesicle exocytosis that would otherwise outpace phasic secretion in response to a rapidly rising Ca^{2+} stimulus. The CpxII N-terminal domain speeds up exocytosis timing by controlling the apparent Ca^{2+} sensitivity of synchronous release, illustrating that distinct domains of CpxII provide synergistic functions to enhance Ca^{2+}-triggered exocytosis. Furthermore, we provide evidence that SytI releases the CpxII clamp at the moment of fusion pore opening, promoting rapid transmitter discharge from single vesicles. Thus, our experiments pinpoint crucial properties of CpxII and SytI that govern SNARE action to meet the speed requirements of regulated exocytosis.

Results

CpxII determines magnitude and kinetics of Ca^{2+}-triggered exocytosis

Synchronous exocytosis in isolated chromaffin cells was recorded by membrane capacitance (CM) measurements using flash photolysis of caged Ca^{2+} (nitrophenyl [NP]-EGTA). Flash-induced changes in intracellular calcium [Ca]i were monitored with a combination of Ca^{2+} indicators (fura-2 and furaptra). The results show that genetic deletion of CpxII strongly diminishes the exocytotic burst (EB) component that is usually observed in response to a stepwise increase in [Ca]i (Fig. 1 A). Both components of the EB, the fast phase (readily releasable pool [RRP]) and the slow phase (slowly releasable pool [SRP]), are similarly affected, but no change in the subsequent sustained rate (SR) is observed (Fig. 1 B). Detailed fitting of the response reveals that the rates of exocytosis from RRP and SRP are slowed (Fig. 1 C). Normalization of the signals confirms the altered kinetic properties of the EB (Fig. 1 D). Furthermore, loss of CpxII confers a longer secretory delay between the stimulus and the onset of the response (Fig. 1, D and E). In addition, CpxII expression in wild-type (wt) cells (wt + CpxII) increases the size of the EB compared with controls expressing GFP (wt + GFP; Fig. 1 A). Both the RRP and the SRP are significantly enhanced, and the SR is reduced (Fig. 1 B), but the kinetic properties of secretion remain unchanged (Fig. 1, C–E). Thus, CpxII is a rate-limiting factor for the magnitude of synchronous exocytosis, and its loss slows the kinetics of stimulus–secretion coupling.

CpxII controls tonic secretion of chromaffin granules

To allow for Ca^{2+}-dependent priming of chromaffin granules, cells are loaded with the NP-EGTA (free [Ca]i = ~500 nM) for 120 s before the flash application while CM, access, and membrane resistance as well as [Ca]i are monitored (Fig. 1 F). Closer analysis of the preflash CM trace shows that intracellular perfusion is accompanied with an increase in CM (142 ± 21 fF, n = 32) in 120 s, which is significantly stronger in CpxII ko cells (326 ± 40 fF, n = 26) and greatly reduced with expression of CpxII in wt cells (16 ± 27 fF, n = 23; Fig. 1, G and H), as recorded at nearly identical [Ca]i (Fig. 1 J). These results indicate that CpxII regulates not only the magnitude of synchronous exocytosis but also controls tonic secretion at submicromolar [Ca]i. A comparison of both types of secretion recorded in the same cells indicates a reciprocal dependence of the EB size on the magnitude of the preceding tonic secretion (r^2 = 0.94; Fig. 1 I). Indeed, the absolute changes in tonic secretion between groups can quantitatively account for alterations in EB size, suggesting that CpxII is specifically required to prevent premature vesicle loss at submicromolar [Ca]i, which would otherwise outpace synchronous secretion.

For comparison, we also studied the impact of a SytI loss on evoked and tonic secretion (Fig. S1). Deletion of SytI specifically reduces the RRP size and lowers the rate of SRP exocytosis,

exocytosis (τ_{RRP} and τ_{SRP}). (D) Normalized CM (as shown in A) scaled to the wt response 1 s after the flash. (inset) Extended scaling of normalized CM during the first 50 ms after flash (arrow) depicting the delayed onset of CpxII secretion. (E) Mean exocytotic delay determined from fitting individual cellular responses. (F–J) CpxII-dependent control of tonic exocytosis determines the EB size. (F) Exemplary recording of CM, series conductance (Gs), membrane conductance (Gm), and [Ca^{2+}]i during infusion of submicromolar [Ca^{2+}]i. A sustained capacitance increase (ΔCM) over 120 s precedes the rapid CM rise in response to the flash-evoked Ca^{2+} increase (arrow). (G) Mean tonic exocytosis determined from the cells shown in A. (H) Rate of tonic exocytosis. (I) Correlation between tonic secretion rate and EB size for the indicated groups. The regression line (r^2 = 0.94) intercepts the y axis (b, y intercept) at 35 fF/10 s (representing ~4 vesicles/s), a value that comes close to the vesicle priming rate at 500 nM [Ca^{2+}]i ($rate_{(500nM)} = 5.35 \times 10^{-3}$/s × 780 unprimed vesicles = 4 vesicles/s; Sørensen, 2004), suggesting that a balance between Ca^{2+}-dependent priming and CpxII-dependent clamping of tonic secretion determines the EB size. (J) The mean preflash [Ca]i values for the tonic CM responses shown in G are nearly identical. *, P < 0.05; **, P < 0.01; ***, P < 0.001, Student's t test versus the corresponding control. Error bars indicate means ± SEM.

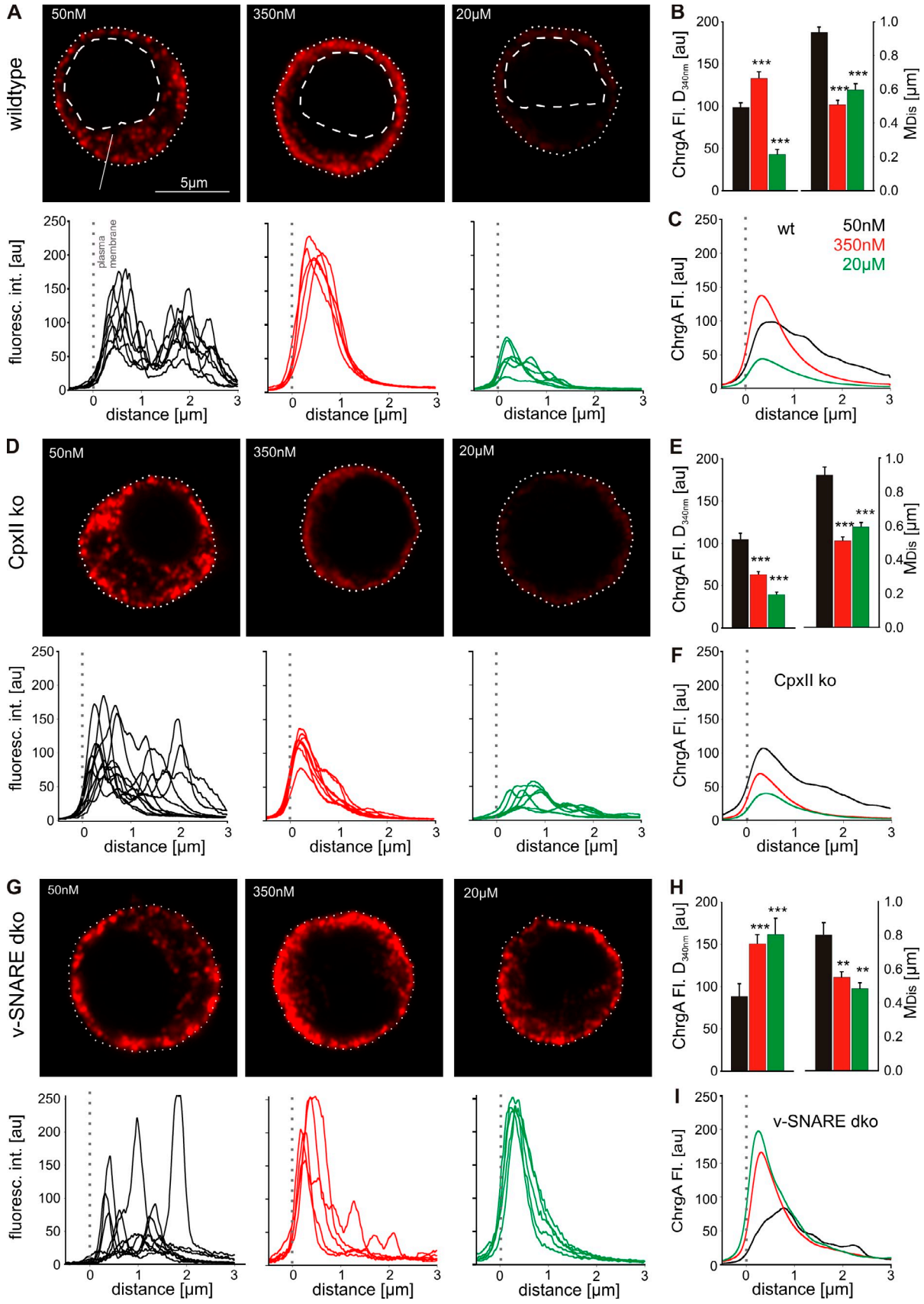

Figure 2. **CpxII hinders premature vesicle release at submicromolar [Ca].** (A) Exemplary images of wt chromaffin cells (permeabilized with 10 µM digitonin) exposed to the indicated [Ca] for 40 s before fixation and immunostaining against the ChrgA (for details see Fig. S2 and Materials and methods). ChrgA staining is scattered throughout the cytoplasm (dashed lines, nuclei) at 50 nM [Ca] (left), concentrated underneath the plasma membrane (dotted

consistent with previous studies (Voets et al., 2001; Nagy et al., 2006). Still, SytI deficiency does not alter tonic secretion, demonstrating that clamping of premature exocytosis is specific for CpxII and not a general feature of SNARE regulators in chromaffin cells (Fig. S1). Furthermore, CpxII expression in SytI ko cells clamps tonic secretion with similar efficiency as in wt cells and leads to a moderate increase in the SRP component. Thus, clamping of tonic exocytosis by CpxII does not depend on SytI in chromaffin cells.

CpxII hinders premature exocytosis at submicromolar [Ca]i

To substantiate the hypothesis that CpxII deficiency leads to vesicle depletion, we analyzed secretion in cells with defined [Ca]i after digitonin permeabilization. The number and distribution of chromaffin granules are determined with confocal microscopy and immunofluorescence using chromogranin A (ChrgA) as a vesicular marker. At 50 nM [Ca]i, ChrgA shows a punctate appearance with scattered distribution throughout the cytoplasm (Fig. 2 A) that is indistinguishable from ChrgA staining of cells not treated with digitonin (Fig. S2) and consistent with the granule distribution determined by electron microscopy (Borisovska et al., 2005; Cai et al., 2008). At 350 nM [Ca]i, however, the immunofluorescence signal is more concentrated in the direct vicinity of the plasma membrane, most likely as a result of Ca^{2+}-dependent reorganization of the actin cortex and vesicle transport toward plasma membrane (Trifaró and Vitale, 1993; Lang et al., 2000). Line scan profiles of the fluorescence signals aligned to the plasma membrane (Fig. 2, A, D, and G, bottom) confirm the redistribution of the ChrgA staining from 50 to 350 nM [Ca]i. The averaged median distance (M_{Dis}) of the immunosignal from the plasma membrane is significantly shorter at 350 nM [Ca]i (0.51 ± 0.02 µm) than at 50 nM [Ca]i (0.94 ± 0.03 µm) and is accompanied by a clear increase in signal amplitude underneath the plasma membrane (Fig. 2, B and C). At 20 µM [Ca]i, the ChrgA signal is strongly reduced because of efficient exocytosis. CpxII ko cells exhibit a similar pattern and distribution of the ChrgA signal for 50 nM (M_{Dis} = 0.9 ± 0.4 µm) and 350 nM [Ca]i (M_{Dis} = 0.51 ± 0.02 µm; Fig. 2, D–F). At 350 nM [Ca]i, however, their staining underneath the plasma membrane is significantly diminished in amplitude (by 40%), indicating premature exocytosis in the absence of CpxII. As a negative control, we used cells that are genetically deficient for SybII and cellubrevin (v-SNARE double ko [dko] cells) and devoid of nearly any secretion (Borisovska et al., 2005). Although these cells indeed fail to promote exocytosis at 20 µM [Ca]i, they exhibit, at 50 and 350 nM [Ca]i, a pattern and reorganization of the ChrgA signal as observed in wt cells (Fig. 2, G–I). Moreover, quantification of the overall cytoplasmic fluorescence signal confirms the similar ChrgA staining for all genotypes at 50 nM [Ca]i and demonstrates the specific and significant loss of ChrgA in CpxII ko cells at 350 nM [Ca]i (Fig. S2). Collectively, CpxII deficiency leads to premature loss of vesicles at submicromolar [Ca]i, as suggested by recordings of tonic exocytosis with CM measurements (Fig. 1). The combined set of data shows that the CpxII-mediated clamp of tonic exocytosis is decisive for the magnitude of synchronous secretion in chromaffin cells.

Distinct domains of CpxII regulate timing and magnitude of synchronous secretion

Encouraged by the aforementioned findings, we studied which CpxII domain regulates stimulus–secretion coupling and clamps premature exocytosis. Interestingly, expression of an N-terminally truncated mutant (ΔN mutant, CpxII aa 28–134; Fig. 3 A) in CpxII ko cells largely restores the EB as seen with CpxII (Fig. 3 B). In contrast, a C-terminally truncated mutant, which lacks the last 62 aa (ΔC mutant, CpxII aa 1–72), almost completely fails to rescue the response. Moreover, the ΔN mutant is unable to restore the kinetics of the EB and the secretory delay, whereas the ΔC mutant rescues the kinetic properties of secretion as does CpxII (Fig. 3, C–F). In close correlation, we find that the ΔC mutant is unable to clamp tonic exocytosis at submicromolar [Ca]i, and the ΔN mutant arrests premature exocytosis with similar efficiency as the wt protein (Fig. 3, G–I). Similar results are observed with expression of the mutant proteins in wt cells (Fig. S3). They confirm the ability of the ΔN mutant to build up a large pool of primed vesicles that fuse with slower kinetics. Inversely, the ΔC mutant suppresses evoked exocytosis of wt cells to the level of CpxII ko cells without changing the kinetic properties. Furthermore, CpxII mutants do not differ from the wt protein regarding the level of protein expression, suggesting that loss of functionally important protein domains causes the observed phenotypes (Fig. S4, C and D). Taken together, the ΔN mutant and the ΔC mutant allow us to uncouple the two functional deficiencies seen in the CpxII ko cells, indicating that distinct domains of CpxII provide separate and autonomous functions for Ca^{2+}-triggered exocytosis.

The CpxII N terminus increases the Ca^{2+} affinity of phasic secretion

For chromaffin cells, timing of fusion events is largely determined by the kinetics of Ca^{2+} binding to SytI serving as the primary Ca^{2+} sensor for exocytosis (Voets et al., 2001; Nagy et al.,

lines) at 350 nM [Ca] (middle), and strongly diminished at 20 µM [Ca] (right). Line scan profiles of ChrgA (aligned to the plasma membrane) are shown below the exemplary images. (B) Amplitude (at 340 nm from the plasma membrane; left) and M_{Dis} of ChrgA signal (right) for the indicated [Ca] in wt cells. Values were determined from the parameter's frequency distribution for each cell (50 nM, *n* = 24; 350 nM, *n* = 24; 20 µM, *n* = 24; data were collected from three independent preparations). (C) Mean line scans illustrate reorganization and loss of the ChrgA signal in wt cells at the indicated [Ca]. Data were collected from the number of cells indicated in B. (D) CpxII ko cells show a significant decrease of ChgrA staining selectively at 350 nM [Ca] compared with controls. int., intensity. (E) Panel organization as in B (50 nM, *n* = 22; 350 nM, *n* = 26; 20 µM, *n* = 26; data were collected from three independent preparations). (F) Mean ChrgA line scans of CpxII ko cells at different [Ca] from the number of cells indicated in E. (G) v-SNARE dko cells fail to secrete at 20 µM [Ca], demonstrating v-SNARE dependence of exocytosis after digitonin permeabilization. (H) Panel organization as in B. (I) Mean ChrgA line scans of v-SNARE dko cells at different [Ca] (50 nM, *n* = 10; 350 nM, *n* = 10; 20 µM, *n* = 10). **, P < 0.01; ***, P < 0.001. Error bars indicate means ± SEM. au, arbitrary unit; Fl., fluorescence.

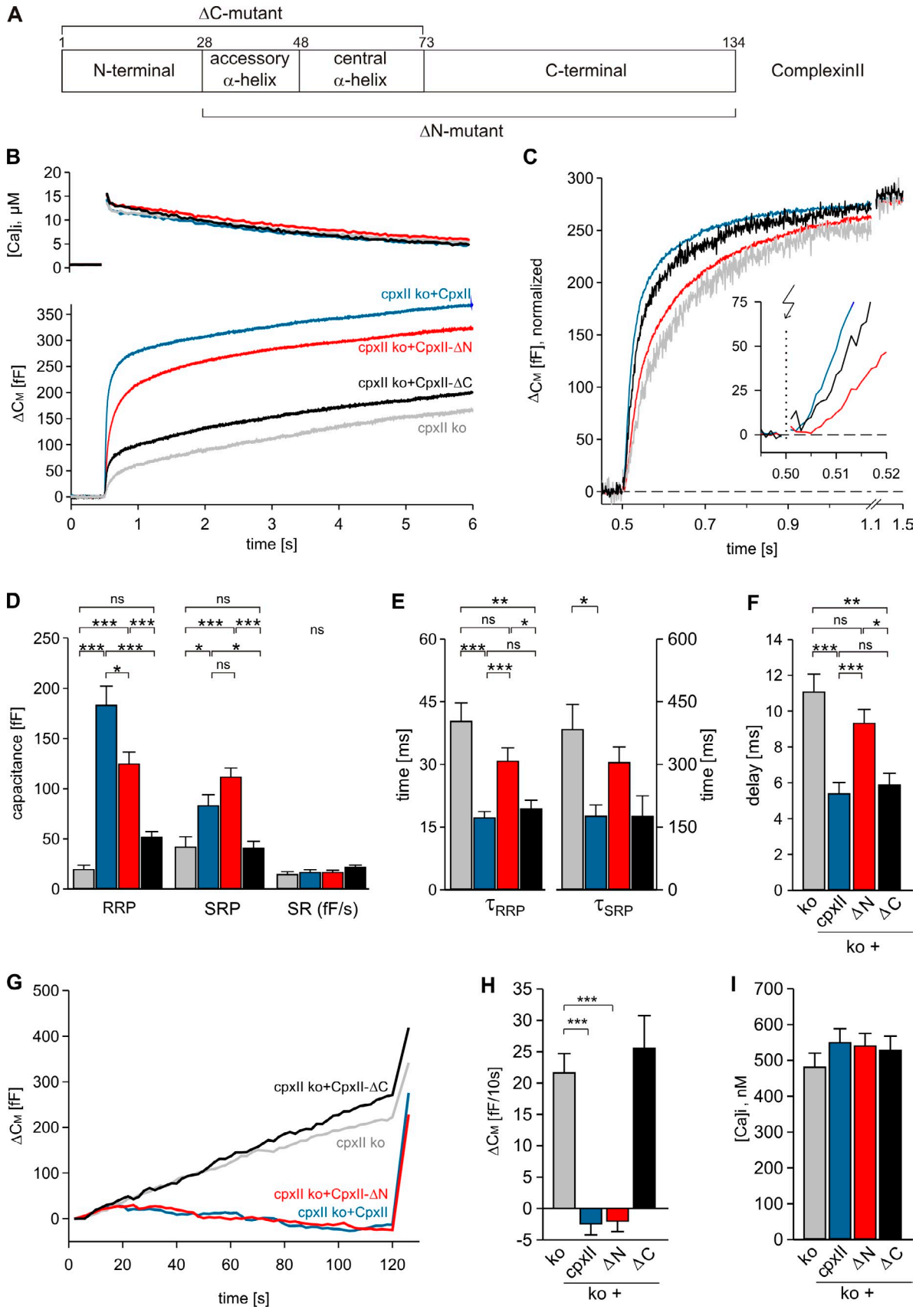

Figure 3. **C- and N-terminal domains of CpxII control extent and time course of secretion.** (A) Schematic view of CpxII domains and its truncated mutants. Numbers, amino acid positions of CpxII. (B) Mean flash-induced $[Ca^{2+}]i$ levels (top) and corresponding CM signals (bottom) of CpxII ko cells (n = 19) and those expressing CpxII (n = 22) or its mutants (CpxII-ΔN, n = 25; CpxII-ΔC, n = 13). Flash, t = 0.5 s. (C) CM signals (as shown in A) normalized to the

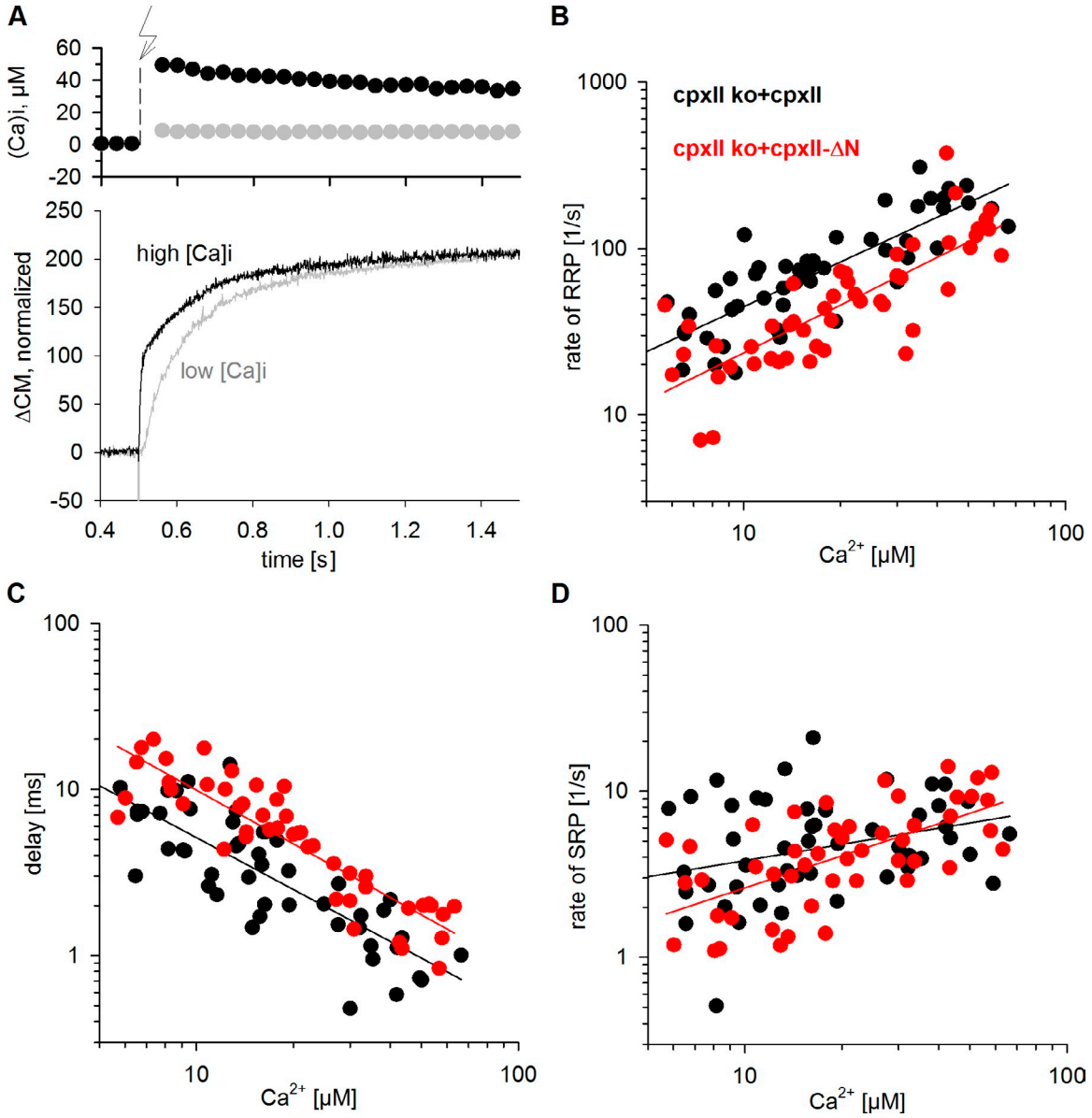

Figure 4. **N-terminal domain of CpxII alters the Ca^{2+} affinity of secretion.** (A) Exemplary recordings of CM signals (bottom) in response to low (gray) and high (black) flash-induced (arrow) [Ca]i levels (top). (B) RRP fusion rate as a function of flash-induced [Ca]i of CpxII ko cells expressing CpxII (n = 47) or the ΔN mutant (n = 49). (C) The onset of ΔN mutant secretion is proportionally longer over the entire range of $[Ca^{2+}]$i. (D) SRP fusion rate of the ΔN mutant does not differ from control at high [Ca]i. Continuous lines show linear regressions.

2006). Consequently, alterations in flash [Ca]i strongly influence the time course of stimulus–secretion coupling (Fig. 4 A). As shown in Fig. 4 B, the rate of RRP exocytosis systematically increases with increasing [Ca]i in CpxII ko cells expressing CpxII. For the ΔN mutant, however, RRP rates are nearly twofold slower over the entire range of investigated Ca^{2+} concentrations. In the same line, the ΔN mutant causes a systematic and proportional increase in the exocytotic delay when compared with controls (Fig. 4 C). Still, for SRP exocytosis, kinetic differences between wt and mutant protein become less apparent at high [Ca]i and are more difficult to determine because the SRP phase is temporally sandwiched between RRP release and the subsequent SR of secretion (Fig. 4 D). Collectively, the results show that the CpxII N terminus accelerates the RRP fusion rate and shortens the exocytotic delay in a Ca^{2+}-dependent fashion. In contrast, extension of the juxtamembrane region of SybII

EB size of the CpxII ko + CpxII response. The inset shows the first 20 ms after flash (arrow), illustrating the delayed onset of CpxII-ΔN–mediated secretion (red) compared with CpxII (blue) and CpxII-ΔC (black). (D–F) Amplitudes of RRP and SRP, the rate of sustained release (SR; femtofarad/second), the time constants of the EB components (τ_{RRP} and τ_{SRP}), and the exocytotic delay determined for CpxII ko (gray), CpxII (blue), CpxII-ΔN (red), and CpxII-ΔC (black). (G) Mean tonic CM responses of the cells shown in B during infusion of submicromolar [Ca]i. (H and I) Rate of tonic exocytosis determined at similar [Ca]i (I) before the flash. *, $P < 0.05$; **, $P < 0.01$; ***, $P < 0.001$. Error bars indicate means ± SEM.

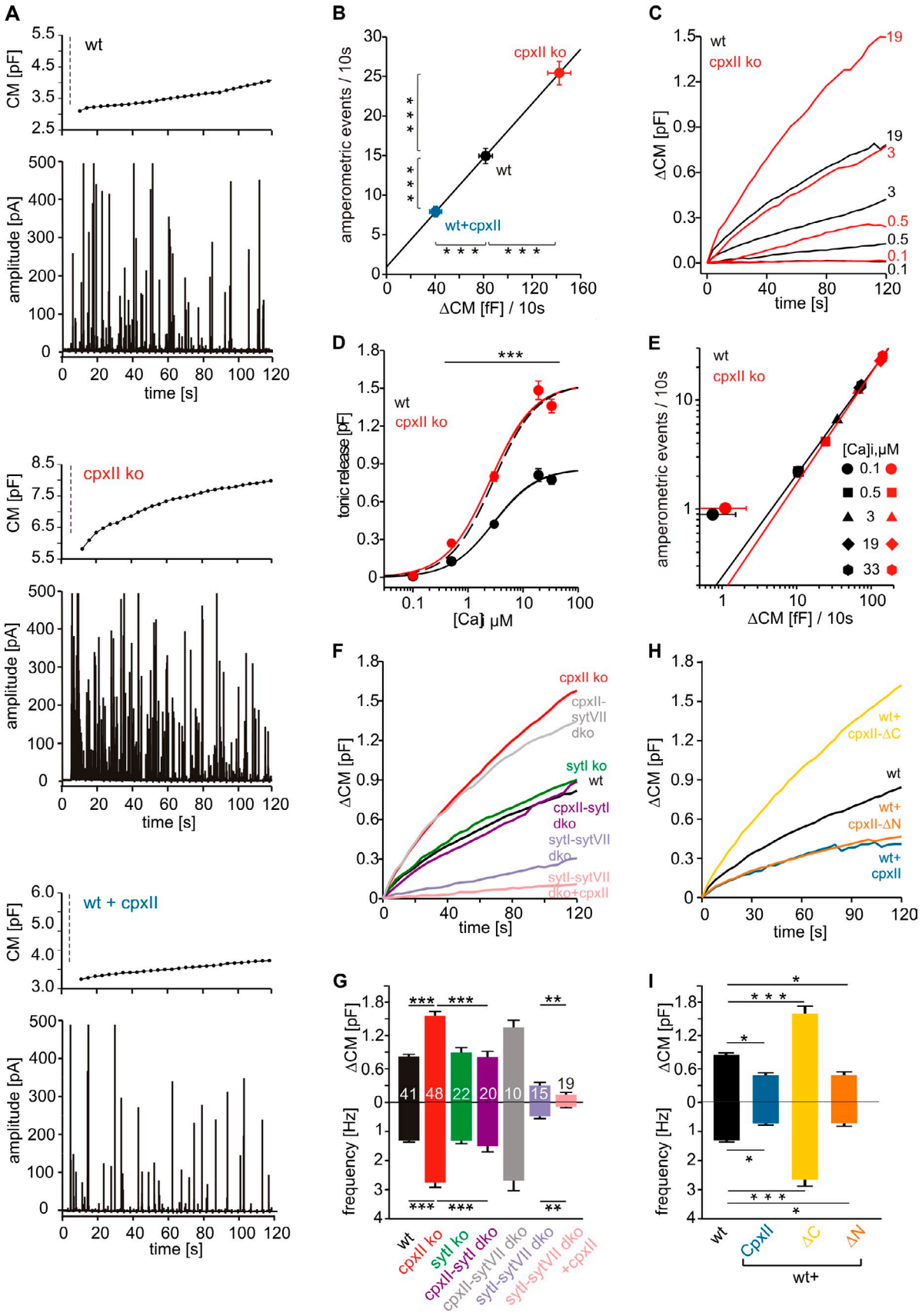

Figure 5. **Inhibitory CpxII and facilitatory SytI control the magnitude of tonic exocytosis.** (A) Exemplary recordings of CM and amperometry for the indicated groups (dashed line, cell opening). (B) The amperometric event frequency scales proportionally to ΔCM at 19 µM [Ca]i (wt, *n* = 38; CpxII ko, *n* = 17; wt + CpxII, *n* = 22). Continuous line, linear regression (r^2 = 0.99; 0.172 events/fF). (C) Ca^{2+} dependence of mean ΔCM in wt and CpxII ko. Numbers

(insertion of an additional 6 aa), which reduces the force transfer on the transmembrane domain, provides a different phenotype by adding a constant time lag of 9 ms to the secretory delay independent of [Ca]i (Kesavan et al., 2007). The proportional changes of RRP fusion rate and delay over the entire range of Ca^{2+} concentrations with the ΔN mutant are characteristic for a decreased Ca^{2+} affinity of synchronous secretion, as will be discussed later (see Discussion). Given these results, we conclude that CpxII provides two synergistic functions for rapid Ca^{2+}-triggered exocytosis in chromaffin cells. It enhances the magnitude of synchronous exocytosis by suppressing a tonic secretion pathway (C terminus) and independently increases the Ca^{2+} affinity of synchronous release (N terminus).

CpxII prevents vesicle depletion at a prepriming stage of exocytosis

To unravel further the mechanism of tonic secretion control by CpxII, exocytosis was stimulated by intracellular perfusion with different [Ca]i and monitored simultaneously with CM measurements and carbon fiber amperometry. Upon stimulation with 19 µM [Ca]i (Fig. 5 A, dashed line), wt cells respond with a strong increase in CM that is accompanied with a barrage of amperometric spikes. Both assays of secretion reveal a significant increase of exocytotic activity in CpxII ko cells and a decrease with CpxII expression in wt cells (Fig. 5, A and B). Intracellular dialysis of wt cells with different [Ca]i shows a Ca^{2+}-dependent increase in tonic exocytosis that reaches its half-maximum activity at 3.27 µM and saturates at concentrations >10 µM [Ca]i (Fig. 5, C and D). In comparison, CpxII ko cells exhibit a similar Ca^{2+} dependency (K_d = 2.72 µM) but show a nearly twofold increase in maximum secretion. The Ca^{2+}-dependent priming reaction, but not the triggering step, is rate limiting for cumulative secretion recorded in chromaffin cells over 100 s (Sørensen, 2004). Because our results provide direct evidence for vesicle depletion rather than enhanced priming in CpxII ko cells (Figs. 1 and 2), the elevated secretion at high [Ca]i indicates premature vesicle exocytosis upstream of the classical priming reaction. No significant differences in exocytotic activity between wt and CpxII ko cells are observed at 100 nM [Ca]i, either with amperometry (wt = 0.9 ± 0.01 events/10 s; CpxII ko = 1.01 ± 0.05 events/10 s) or with CM measurements (wt = 0.7 ± 0.8 fF/10 s; CpxII ko = 1.1 ± 1 fF/10 s; Fig. 5, D and E), confirming our observations with ChrgA release (Fig. 2). Furthermore, the close correlation between ΔCM and amperometric event frequency (r^2 = 0.99; slope = 0.172 events/fF) agrees well with the theoretical relationship between both measurements (for details, see Materials and methods) and indicates that the observed CM changes are caused by alterations in granule exocytosis rather than in endocytosis (Fig. 5 B). Thus, neither loss nor overexpression of CpxII changes the mode of exocytosis, leading to premature closure of the fusion pore, as suggested earlier (Archer et al., 2002; An et al., 2010). For both wt and CpxII ko, amperometric event frequency also correlates strictly with ΔCM over [Ca]i ranging from 0.5 to 33 µM but deviates at 100 nM [Ca]i (Fig. 5 E). The higher frequency of amperometric events relative to ΔCM (at 100 nM $[Ca]_i$) is accompanied with a smaller event charge (wt = 106 ± 13 fC, n = 21; CpxII ko = 91 ± 9 fC, n = 20) and a threefold reduction in amplitude (wt = 29.9 ± 4 pA; CpxII ko = 24 ± 3 pA), when compared with recordings at 19 µM [Ca]i (Fig. S4 A). This phenotype may result from incomplete transmitter discharge as a result of premature fusion pore closure at low [Ca]i (Fulop et al., 2005) but is unchanged in CpxII ko. Taken together, CpxII action prevents vesicle depletion at a prepriming stage but does not change the mode of exocytosis.

CpxII controls the rate of tonic secretion independently of SytI and SytVII

Previous results in hippocampal neurons have suggested that CpxII clamps asynchronous release by blocking a secondary Ca^{2+} sensor (Yang et al., 2010; also see Neher, 2010). Because chromaffin cells are equipped with two functionally overlapping Ca^{2+} sensors, SytI and SytVII (Wang et al., 2005; Schonn et al., 2008; Segovia et al., 2010), we comparatively analyzed tonic secretion of single ko (CpxII ko and SytI ko) and dko animals (CpxII-SytI dko, CpxII-SytVII dko, and SytI-SytVII dko). Enhanced tonic secretion with loss of CpxII is strongly reduced in the additional absence of SytI (CpxII-SytI dko; Fig. 5, F and G), showing that SytI still acts as the predominant Ca^{2+} sensor under these conditions. The combined absence of CpxII and SytVII (CpxII-SytVII dko) does not alter the CM response, confirming the specific requirement of SytI for elevated tonic exocytosis of CpxII ko cells (Fig. 5, F and G). Although tonic secretion is unaffected in the sole absence of SytI, it is greatly reduced in SytI-SytVII dko cells, indicating redundant functions of both Syt isoforms in facilitating granule exocytosis (also see Schonn et al., 2008). Furthermore, CpxII expression reduces the ΔCM remaining in SytI-SytVII dko cells with similar efficacy as in wt cells (SytI-SytVII dko = 301 ± 55 fF; SytI-SytVII dko + CpxII = 136 ± 40 fF; wt = 921 ± 65 fF; wt + CpxII = 420 ± 49 fF), showing that CpxII clamping depends neither on SytI nor on SytVII (Fig. 5, F–I). Analogous to secretion at submicromolar [Ca]i (Fig. S3), expression of the ΔN mutant in wt cells reduces even high rates of tonic secretion like CpxII, whereas the ΔC mutant

indicate [Ca]i in micromolars. t = 0, first CM measurement. (D) Tonic ΔCM as a function of [Ca]i for wt and CpxII ko. Data were approximated with Hill's equation (maximum secretion [Smax]: wt = 863 fF and CpxII ko = 1,533 fF; K_d: wt = 3.27 µM and CpxII ko = 2.72 µM; Hill coefficient, n: wt = 1.10 and CpxII ko = 1.08) and averaged from a total of 88 wt and 91 CpxII ko cells. Dashed line, normalized wt response. ***, P < 0.001, Student's t test versus wt at the corresponding [Ca]i. (E) Amperometric event frequency correlates with the corresponding ΔCM for wt and CpxII ko at [Ca]i ranging from 0.5 to 33 µM. Continuous line, linear regression for [Ca]i between 0.5 and 33 µM (wt = 0.18 events/fF, r^2 = 0.99; CpxII ko = 0.175 events/fF, r^2 = 0.99). (F) Mean CM responses upon perfusion with 19 µM [Ca]i in wt, CpxII ko, SytI ko, SytI/CpxII dko, SytVII/CpxII dko, SytI/SytVII dko, and SytI/SytVII dko cells expressing CpxII. (G) Total ΔCM after 120 s (top) and amperometric event frequency (bottom). Numbers of cells are depicted in the bars. **, P < 0.01; ***, P < 0.001, Student's t test versus control. (H) The ΔN mutant (n = 17) clamps tonic exocytosis (at 19 µM [Ca]i) like CpxII (n = 19), whereas the ΔC mutant (n = 19) unclamps exocytosis to the level of CpxII ko cells when expressed in wt cells (n = 17). (I) Mean ΔCM after 120 s (top) and amperometric event frequency (bottom) for the data shown in H. *, P < 0.05; **, P < 0.01; ***, P < 0.001. Error bars indicate means ± SEM.

enhances exocytosis to the level of CpxII ko (Fig. 5, H and I). Collectively, CpxII interferes with tonic secretion independently of SytI or SytVII. Because another auxiliary Ca^{2+} sensor, the Ca^{2+} binding protein Doc2b (Verhage et al., 1997; Groffen et al., 2010), does not regulate exocytosis of chromaffin cells in the low micromolar calcium range (Pinheiro et al., 2013), it is likely that CpxII directly clamps the underlying SNARE-mediated fusion mechanism.

Balanced action of CpxII and SytI determines the initial fusion pore kinetics

A key toward the understanding of CpxII action in exocytosis is to determine the time point when CpxII clamping is released. To study whether CpxII action can be detected even after fusion initiation, we analyzed the properties of single vesicle release in detail. Amperometric spikes were characterized with respect to amplitude and kinetics of the main spike and the prespike signal, the latter reflecting neurotransmitter efflux from the vesicle through a narrow fusion pore (Chow et al., 1992; Bruns and Jahn, 1995). Comparison of the frequency distributions for the indicated parameters (Fig. 6 A) and of the cell-weighted averages (Fig. S4, A and B) shows that loss of CpxII affects neither the main spike phase regarding its charge, amplitude, or kinetics nor the magnitude or timing of the prespike signal at 19 µM [Ca]i (Fig. 6, A–D). Loss of SytI, however, strongly increases prespike duration and charge, as depicted for exemplary events (Fig. 6 B). Interestingly, the delayed fusion pore expansion seen in SytI ko is fully compensated by additional absence of CpxII in SytI-CpxII dko, showing that CpxII contributes to lengthening of the prespike signal in the absence of SytI. This result together with the similar fusion pore phenotype of wt and CpxII ko suggests that SytI functionally antagonizes the inhibitory CpxII action on fusion pore dilation in wt cells. In good agreement, CpxII expression in wt prolongs the fusion pore expansion time and increases the prespike charge without changing amplitude or kinetics of the main spike (Fig. 6, A–D). Thus, CpxII overexpression reproduces the SytI ko phenotype, confirming that competitive actions of SytI and CpxII determine initial fusion pore kinetics. Given the involvement of SytI in the regulation of the prespike signal, we studied the effects of different [Ca]i in wt cells (Fig. 6 E). Reducing [Ca]i from 19 to 3 µM and further to 500 nM gradually prolongs the fusion pore expansion time and increases the prespike charge. This observation agrees with results from mast and PC12 cells (Fernández-Chacón and Alvarez de Toledo, 1995; Wang et al., 2006) and is compatible with a Syt-mediated control of fusion pore dilation (Wang et al., 2001, 2003, 2006; Bai et al., 2004; Lynch et al., 2008; Segovia et al., 2010). In contrast to 19 µM[Ca]i, CpxII loss significantly shortens the prespike signal (and decreases its charge) when lowering [Ca]i, unmasking a Ca^{2+}-dependent change in the balance between SytI and CpxII action toward an enhanced CpxII clamp (Fig. 6 E). The CpxII R63A mutant, which is unable to bind SNARE complexes (Xue et al., 2007) and has similar expression as CpxII (Fig. S4, C and D), fails to suppress tonic secretion and to stabilize the exocytotic fusion pore. This shows that unperturbed SNARE binding is essential for CpxII to exert both functions (Fig. S5). Taken together, these results provide direct evidence for the interplay of SytI and CpxII in controlling fusion pore dynamics. They illustrate that CpxII-mediated stabilization of the early fusion pore is efficiently antagonized at high [Ca]i by SytI at the moment of fusion pore opening.

CpxII controls the fusion pore jitter

Prespike signals often exhibit fast fluctuations that clearly exceed the baseline noise and may reflect attempts of the SNARE machinery to widen the initial fusion pore (Kesavan et al., 2007). Diminished fluctuations, as observed with SybII mutants carrying an extended juxtamembrane region (linker mutants), are most likely caused by reduced force transfer between the complex-forming SNARE motif and the transmembrane domain. With loss of CpxII, the frequency of prespike fluctuations is not altered (CpxII ko = 0.34 ± 0.03 kHz; wt = 0.32 ± 0.02 kHz) but is significantly reduced in SytI ko (0.20 ± 0.02 kHz), an effect, which is fully abrogated in the combined absence of SytI and CpxII (0.3 ± 0.02 kHz; Fig. 7, A and B). Moreover, CpxII expression in wt cells generates a phenotype that resembles closely that of SytI ko cells (P = 0.84). As shown in Fig. 7 D, the number of fluctuations increases linear to the prespike duration (wt = 0.3 fluctuations/ms; $r^2 = 0.87$) and is significantly reduced over the entire range of prespike durations for SytI ko (0.2 fluctuations/ms; $r^2 = 0.8$) and for CpxII overexpression (0.2 fluctuations/ms; $r^2 = 0.8$). Thus, changes in fluctuation frequency are not simply a consequence of lengthening the fusion pore expansion time in SytI ko and wt + CpxII cells. Analysis of the root–mean–square (rms) noise of the prespike's current derivative, serving as a threshold-independent parameter of fusion pore fluctuations, corroborates that both SytI loss and CpxII expression significantly reduce the fusion pore jitter (Fig. 7, C and E). Moreover, expression of the ΔN mutant, which averts tonic secretion in wt cells (Fig. 5, H and I), significantly prolongs the prespike signal (wt + ΔN = 9.2 ± 0.51 ms, $n = 17$, $P < 0.001$) and reduces pore fluctuations like CpxII (Fig. 7, A–C). In contrast, the ΔC mutant, which "unclamps" tonic secretion, fails to affect duration (wt + ΔC = 4.27 ± 0.35 ms, $n = 19$, P = 0.81) and dynamics of the early fusion pore. Thus, the CpxII C terminus actively controls the extent of tonic secretion and the speed of fusion pore expansion. The effects of CpxII expression on high frequency oscillations of the prespike signal are abolished with the SNARE binding mutant R63A (Fig. S5) and are remarkably similar to those of SybII linker mutants (Fig. 7, B–D). In summary, CpxII clamps SNAREs with its C-terminal domain and thereby reduces their force transfer on fusing membranes, a mechanism that prevents premature exocytosis and stabilizes the early fusion pore.

Discussion

Spontaneous SNARE protein assembly requires mechanisms that allow for synchronization of SNARE activity at the moment of the Ca^{2+} rise. Our experiments show for the first time how distinct domains of CpxII function synergistically to fulfill this task, on one hand by suppressing premature secretion leading to a concomitant increase in synchronized exocytosis and on the

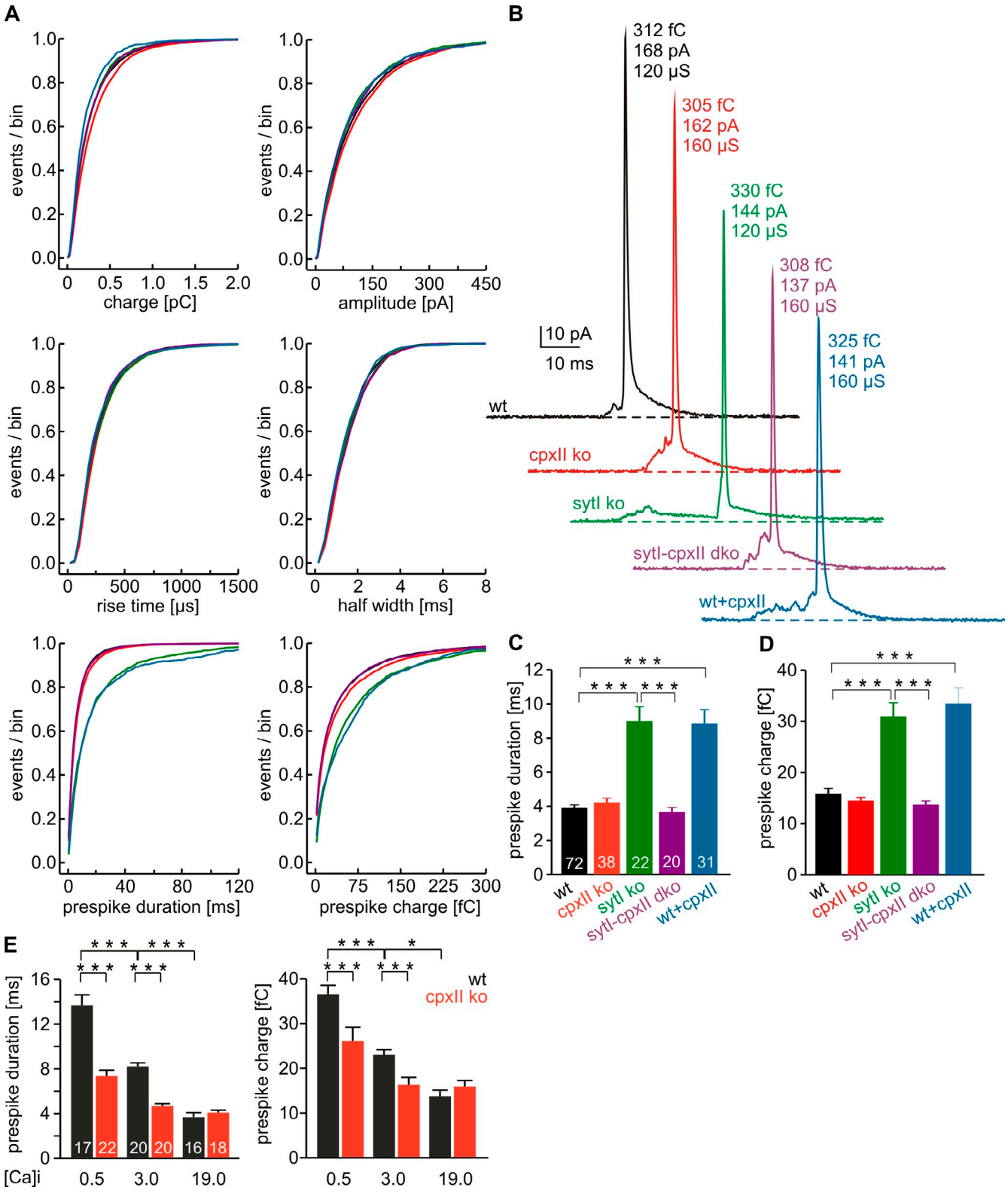

Figure 6. **SytI-CpxII antagonism determines fusion pore dynamics.** (A) Properties of the main amperometric spikes and their prespike signals, displayed as cumulative frequency distribution for the indicated parameters. Data were collected from the following genotypes (number of events): wt (black; 8,350), CpxII ko (red; 6,051), SytI ko (green; 2,051), CpxII-SytI dko (purple; 2,431), and wt + CpxII (blue; 1,815). (B) Exemplary single-release events with similar charge and 50–90% rise time for wt, CpxII ko, SytI ko, CpxII-SytI dko, and wt + CpxII. (C and D) SytI absence increases fusion pore expansion time and prespike charge, both of which are restored by additional loss of CpxII. CpxII expression in wt cells mimics the SytI ko phenotype. Values are given as means of the median determined from the parameter's frequency distribution for each cell. Numbers of cells are depicted in the bars (>40 events/cell). (E) Dependence of the prespike duration (left) and charge (right) on the indicated [Ca]i (micromolars) for wt and CpxII ko. Numbers of cells are depicted in bars. *, $P < 0.05$; ***, $P < 0.001$, Student's *t* test for comparison between groups at the same [Ca]i in E. Error bars indicate means ± SEM.

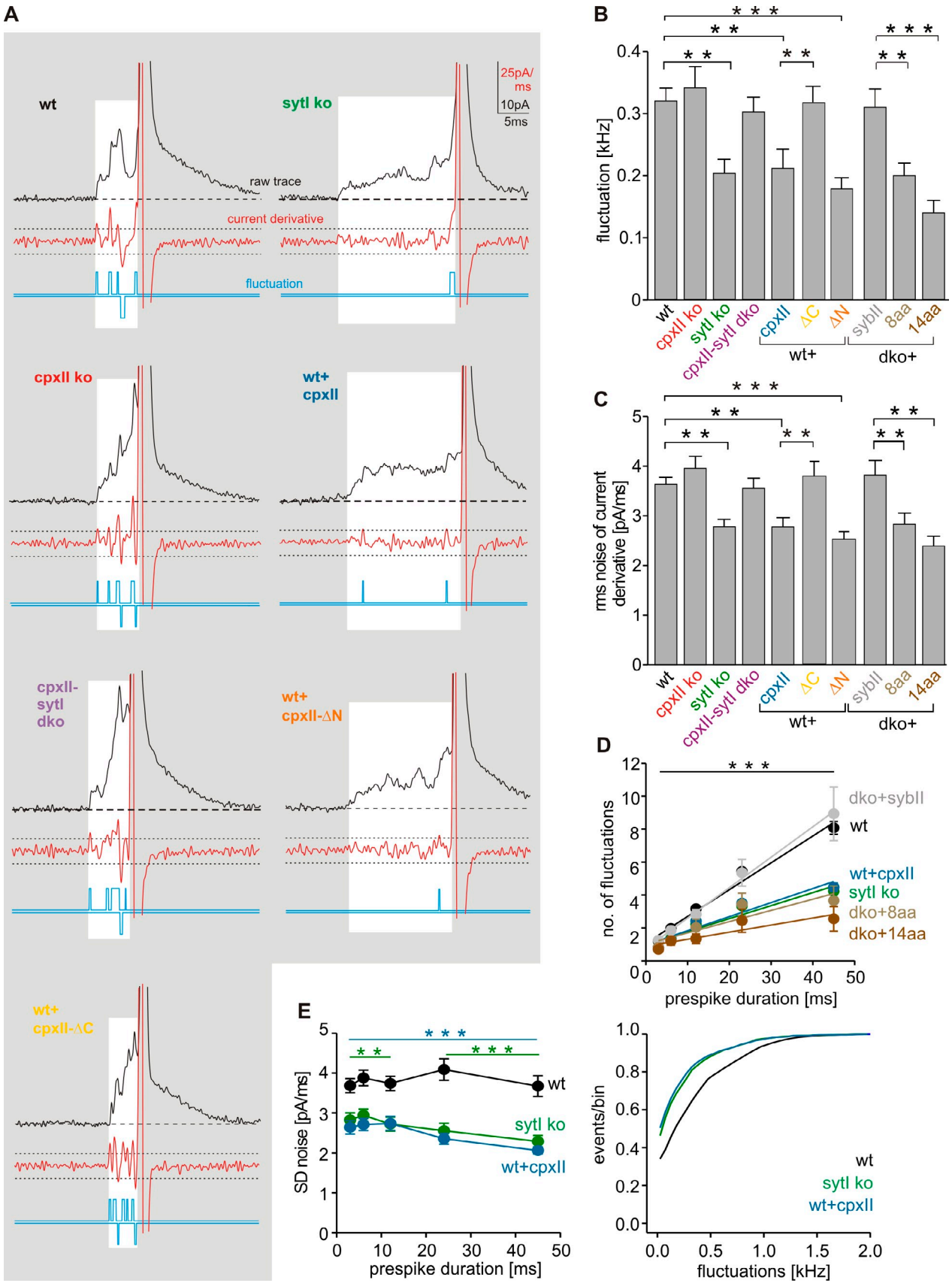

Figure 7. **CpxII controls the fusion pore jitter.** (A) Exemplary analyses of current fluctuations during the prespike phase (highlighted area). Deflections of the current derivative (red traces) beyond the threshold (dashed lines = ±4 SD of baseline noise) were counted as fluctuations (blue traces). The displayed events have a similar charge and 50–90% rise time (wt: 348 fC and 160 µs; Sytl ko: 303 fC and 160 µs; CpxII ko: 323 fC and 200 µs; CpxII-Sytl dko:

other hand by increasing the Ca^{2+} affinity of exocytosis, leading to faster stimulus–secretion coupling. Using a combination of null mutants for CpxII and SytI, we illustrate the interplay of both proteins in controlling fusion pore dynamics and demonstrate that SytI antagonizes the CpxII clamp at the moment of the Ca^{2+} rise, enabling bona fide transmitter release from single vesicles. Thus, these experiments show how CpxII and the primary Ca^{2+} sensor SytI guide SNARE-mediated exocytosis in a functional pas de deux from pre- to postfusional stages.

CpxII enhances synchronous secretion by preventing premature vesicle depletion

Most previous ko and knockdown studies of Cpx agreed on the point that its absence reduces evoked exocytosis but suggested inconsistent mechanisms for the loss-of-function phenotype, such as a general loss of exocytosis activation (Reim et al., 2001; Tang et al., 2006; Xue et al., 2007, 2008, 2009; Strenzke et al., 2009; Cho et al., 2010; Martin et al., 2011; Jorquera et al., 2012; Cao et al., 2013), reduced priming of vesicles (Yang et al., 2010; Kaeser-Woo et al., 2012; Lin et al., 2013), their depletion (Hobson et al., 2011), or changes in vesicle fusogenicity (Maximov et al., 2009; Xue et al., 2010). In particular, it remained unclear to what extent elevated asynchronous release, as observed in several studies (e.g., Yang et al., 2010; Jorquera et al., 2012), leads to depletion of the vesicle pool that supports evoked release. Secretion analyses in chromaffin cells allow for a direct and quantitative comparison of tonic and evoked exocytosis recorded from the same set of cells in front of a well-defined [Ca]i. We find that CpxII loss in chromaffin cells causes significant tonic release at elevated resting levels of [Ca]i (>100 nM) and a concomitant decrease of the flash-induced synchronous response. Furthermore, CpxII expression strongly enhances evoked exocytosis by nearly abolishing any tonic secretion at submicromolar [Ca]i. The inverse relationship between both types of secretion indicates that CpxII-controlled tonic exocytosis can outpace synchronous secretion. These results indicate that CpxII hinders depletion of exocytosis-competent vesicles and does not facilitate priming as has been suggested earlier (Cai et al., 2008; Yang et al., 2010; Kaeser-Woo et al., 2012; Lin et al., 2013). By studying ChrgA release at defined [Ca]i, we verify that loss of CpxII produces significant vesicle exocytosis at 350 nM [Ca]i, providing independent evidence for the depletion phenotype. Given that CpxII deficiency enhances the rate of tonic secretion at 20 µM [Ca]i but lowers the fusion rate of primed vesicles at a similar [Ca]i, as observed in our flash experiments, we conclude that CpxII preferentially clamps an autonomous tonic secretion pathway branching off upstream of vesicle priming (Fig. 8). Collectively, CpxII is rate limiting in the control of premature granule exocytosis and thereby determines the magnitude of synchronous secretion.

CpxII C terminus hinders SNAREs instead of a putative secondary Ca^{2+} sensor

Previous work on hippocampal neurons suggested that loss of Cpx increases the frequency of spontaneous miniature excitatory postsynaptic current by unclamping a putative secondary Ca^{2+} sensor (Yang et al., 2010). Our results are difficult to reconcile with such a scenario in chromaffin cells. First, we show that loss of SytI, but not of SytVII, abrogates elevated tonic exocytosis seen in the absence of CpxII, indicating that SytI remains the main Ca^{2+} sensor of secretion also in CpxII ko cells. Second, tonic secretion of CpxII-null mutants exhibits the same Ca^{2+} dependency as wt cells, providing no evidence for the involvement of an alternative Ca^{2+} sensor with altered Ca^{2+} binding properties. Thus, elevated secretion in CpxII ko requires the function of the primary Ca^{2+} sensor SytI. This does not necessarily mean that CpxII clamps SytI, e.g., by regulating its access to SNAREs (Jorquera et al., 2012). In contrast, we find that CpxII overexpression in SytI ko and also in SytI/SytVII dko cells suppresses tonic exocytosis with similar efficiency as in wt cells. Furthermore, experiments with the R63A mutant demonstrate that SNARE binding is a prerequisite for inhibitory action of CpxII. Collectively, these results favor a molecular mechanism wherein CpxII hinders SNARE activity directly and thereby stalls tonic secretion.

Recent experiments at the NMJ of *C. elegans* suggested that the CpxII C-terminal domain tethers the protein via its amphipathic helix to synaptic vesicles and thus concentrates the SNARE-binding region at the site of exocytosis for efficient clamping (Wragg et al., 2013). Our experiments in chromaffin cells disagree with a simple targeting role of the Cpx C terminus. CpxII-ΔC impairs synchronized exocytosis in wt cells and actively unclamps tonic secretion to the level of the CpxII ko phenotype. These observations indicate that the ΔC mutant competes with endogenous CpxII for binding to productive SNARE complexes but has lost its ability to clamp tonic secretion. Thus, the C terminus actively suppresses premature exocytosis, a property that may also rely on lipid binding of this protein domain (Seiler et al., 2009; Kaeser-Woo et al., 2012; Wragg et al., 2013). Given that the accessory α helix is thought to be involved in inhibiting SNARE-mediated fusion (Giraudo et al., 2006, 2008, 2009; Schaub et al., 2006; Xue et al., 2007; Yoon et al., 2008; Maximov et al., 2009; Kümmel et al., 2011),

312 fC and 200 µs; wt + CpxII: 334 fC and 160 µs; wt + CpxII-ΔC: 307 fC and 160 µs; wt + CpxII-ΔN: 335 fC and 200 µs), indicating that differences in fluctuations are not a consequence of diffusional smearing. (B) Mean fluctuation frequency (positive and negative fluctuations) of the prespike signal for the indicated ko cells, wt cells expressing CpxII, or its mutant variants and v-SNARE dko cells expressing SybII or a linker mutant. Data for SybII and its mutants carrying an extended juxtamembrane domain (plus 8 or 14 aa: dko + SybII-8aa and dko + SybII-14aa) are taken from Kesavan et al. (2007). Data were averaged from the number of cells indicated in Figs. 6 C and 5 H. (C) rms noise of the current derivative during the prespike. (D) Number of fluctuations increases with longer prespike duration and is significantly reduced over the entire range of prespike durations in SytI ko, wt + CpxII, and v-SNARE dko cells expressing the SybII linker mutants. (E) rms noise plotted as a function of prespike duration (left) and fluctuation frequency as cumulative frequency distribution (right). Data were collected from the following number of cells (prespike signals): wt, 41 (3,503); SytI ko, 22 (1,626); and wt + CpxII, 21 (815). **, $P < 0.01$; ***, $P < 0.001$, Student's *t* test versus control at the corresponding prespike duration in D and E. **, $P < 0.01$; ***, $P < 0.001$, in B and C. Error bars indicate means ± SEM.

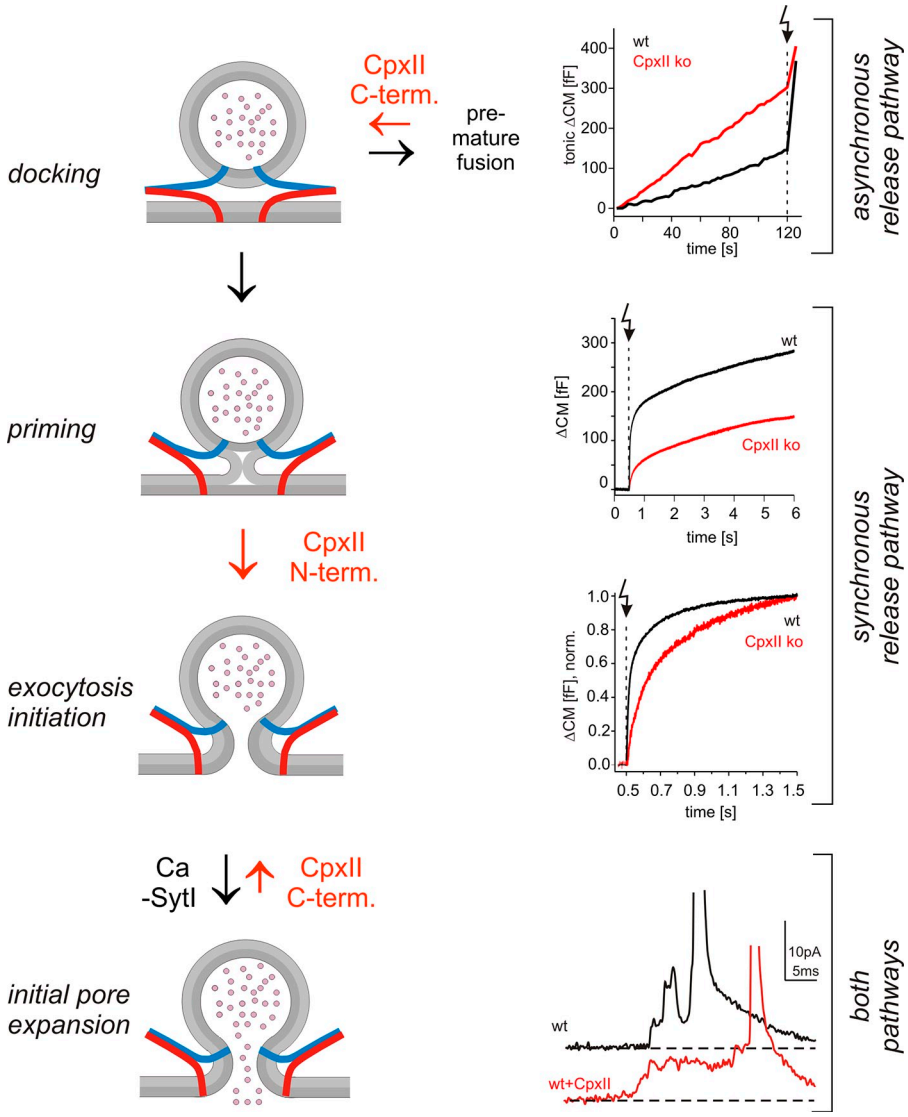

Figure 8. **Hypothetical model of Cpx action in vesicle exocytosis.** The CpxII C terminus hinders premature fusion of docked vesicles through an asynchronous pathway and thereby increases the primed vesicle pool. Additionally, its N terminus speeds up fusion of primed vesicles, providing two independent, synergistic functions of CpxII to enhance synchronous release. Clamping of premature exocytosis by CpxII C terminus is continued from docking until fusion pore opening, most likely by hindering SNARE assembly (v-SNAREs, blue; t-SNAREs, red). Ca-bound SytI efficiently releases the clamp upon fusion pore opening in wt cells, as suggested by the Syt ko phenotype, CpxII overexpression, and experiments with lowered [Ca]i (Fig. 6). Arrow (dotted line) indicates flash. norm., normalized; term., terminus.

an attractive explanation could be that the CpxII C terminus folds back on this protein region and promotes with its amphipathic helix both protein–lipid and protein–protein interactions to stabilize the position of the accessory α helix on the SNARE complex.

CpxII N terminus speeds up fusion of primed vesicles

CpxII deficiency in chromaffin cells is characterized by delayed and slower stimulus–secretion coupling, a phenotype that can be reproduced in isolation by expressing the ΔN mutant in CpxII ko (Fig. 3) or wt cells (Fig. S3). Previous results with Cpx ko neurons and those expressing a similar Cpx-ΔN mutant (CpxII aa 16–134) showed a greater potentiation of the excitatory postsynaptic current amplitude upon elevation of extracellular [Ca] than wt neurons (Xue et al., 2007, 2010). Our direct analysis of secretion rates as the function of [Ca]i reveals that loss of the CpxII N terminus shifts the Ca^{2+} dependence of RRP rate and secretory delay to higher [Ca]i. This behavior is characteristic for a decreased forward rate of Ca^{2+} binding and is remarkably similar to the phenotype of a SytI mutant (R233Q) with lowered Ca^{2+} affinity (Sørensen et al., 2003). Because CpxII lacks any Ca^{2+} binding sites, it may serve with its N terminus as an adaptor for the Ca^{2+} sensor SytI (see also Neher, 2010), changing its Ca^{2+} affinity either by direct interaction or indirectly by lowering the energy level for Ca^{2+}-triggered fusion through concurrent SNARE binding (Chicka and Chapman, 2009; Xu et al., 2013). Yet, a SytI-independent change in the Ca^{2+} affinity of secretion by CpxII cannot be excluded. Based on our results, it is tempting to speculate that the facilitatory role of CpxII and its N terminus on evoked release in hippocampal neurons as well as the slower rise time of the evoked endplate response observed at the NMJs of Cpx-null mutants (Jorquera et al., 2012; Lin et al., 2013) are largely caused by changes in the Ca^{2+} affinity of secretion because action potential evoked release requires fast stimulus–secretion coupling. Although previous studies have emphasized antagonistic roles (facilitatory and inhibitory) of Cpx (e.g., Maximov et al., 2009; Xue et al., 2009), our results provide a new insight by highlighting two independent functions of CpxII that synergize to enhance synchronous release (Fig. 8).

SytI-CpxII antagonism controls fusion pore dynamics

Biochemical experiments have proposed that release of Cpx inhibitory activity by binding of SytI to the SNARE complex causes Cpx displacement and exocytosis triggering (Tang et al., 2006). Still, the validity of this Syt/Cpx switch model was questioned based on simultaneous binding of Cpx and SytI to SNARE complexes (Chicka and Chapman, 2009; Xu et al., 2013). In particular, direct evidence for hallmarks of the hypothesis that these proteins antagonize each other in vivo during membrane fusion has not been presented. We demonstrate that loss of SytI prolongs the fusion pore expansion time, an effect that is fully countered by additional absence of CpxII. Furthermore, overexpression of CpxII in wt cells hinders fusion pore expansion and reproduces the SytI ko phenotype, illustrating competitive actions of both proteins in controlling fusion pore dynamics. Although CpxII deficiency has no impact on the fusion pore at high [Ca]i, it increasingly speeds up fusion pore dilation with lowering [Ca]i, demonstrating opposite effects of CpxII loss and overexpression on fusion pore dynamics in wt cells. The different effect of CpxII deficiency on fusion pore dynamics at low and high [Ca]i is best explained in the context of a SytI/CpxII antagonism, wherein a SytI/Ca^{2+}-mediated acceleration of fusion pore dilation counteracts CpxII clamping and is maximal at high [Ca]i. These results demonstrate the interplay of both proteins at the resolution level of the exocytotic fusion pore and provide the first evidence that SytI antagonizes CpxII action (directly or indirectly) at the moment of fusion pore opening to enable rapid transmitter discharge from individual vesicles (Fig. 8).

Our observations show that SytI deficiency alters fusion pore lifetime but not the overall secretion rate, suggesting that these processes represent two distinct steps in membrane fusion. Importantly, the same domain of CpxII, the C terminus that stalls tonic secretion, also hinders fusion pore expansion. This suggests that CpxII clamps vesicle exocytosis from a preprimed stage to fusion pore opening by similar mechanisms. Furthermore, enhanced CpxII action diminishes fluctuations of the early fusion pore and mimics the phenotype of SybII linker mutations (Kesavan et al., 2007), indicating interference with the SNARE machinery and its force contribution to membrane fusion. In this context, it is important to note that SybII linker mutants additionally slow down the rapid phase (spike) of transmitter discharge (Kesavan et al., 2007), suggesting a sequence of molecular steps, in which SNARE regulators keep control of SNAREs up to the early phase of fusion pore expansion, whereas SNARE action is continued throughout the final, rapid expansion of the pore.

Collectively, our results delineate a pattern of synergistic CpxII actions in Ca^{2+}-triggered exocytosis. They illustrate that the CpxII C terminus is instrumental in clamping SNARE-mediated tonic exocytosis, leading to a corresponding increase of synchronous secretion. The N terminus of CpxII accelerates stimulus–secretion coupling and increases the Ca^{2+} affinity of phasic release, potentially by adapting the major Ca^{2+} sensor SytI. Furthermore, they provide direct evidence that SytI action overcomes CpxII-mediated restraints on force transduction at the moment of fusion pore opening, leading to rapid transmitter release from single vesicles.

Materials and methods

Mutant mice and cell culture

Experiments were performed on embryonic mouse chromaffin cells prepared at embryonic day 17.5 (E17.5)–E18.5. SytI ko animals (Geppert et al., 1994), provided by T. Sudhof (Stanford University, Stanford, CA), were generated by replacing the 5′ portion of the exon encoding aa 270–308 and the preceding intron with a neomycin selection cassette. SytVII ko mice were purchased from The Jackson Laboratory. For generation of SytVII ko animals, a 4.2-kb genomic fragment containing exons 4 and 5 was replaced with a loxP-flanked neomycin resistance gene expression cassette (Chakrabarti et al., 2003). CpxII ko animals were generated by replacing all exons encoding for the open reading frame of CpxII with a neomycin resistance cassette (Reim et al., 2001). Double-deficient mouse lines were generated by crossbreeding SytI or SytVII heterozygosity onto a CpxII homozygous null background. Corresponding double-null mutants were recovered at the expected Mendelian ratio. Chromaffin cells were cultured as described by Borisovska et al. (2005). In brief, embryonic adrenal glands were removed after caesarean section, placed in ice-cold Locke's solution (154 mM NaCl, 5.6 mM KCl, 3.6 mM $NaHCO_3$, 5 mM Hepes, and 5.6 mM glucose, pH 7.3), and cleaned of connective tissue. After enzyme treatment (15 U/ml papain; Worthington Biochemical Corporation) for 30 min, glands were triturated, and cells were cultured at 37°C and 9% CO_2 in enriched DMEM (100 ml DMEM supplemented with 0.4 ml penicillin/streptomycin and 1 ml insulin-transferrin-selenium-X; Invitrogen). Recordings were performed at room temperature on days 1–3 in culture and 4.5–5.5 h after infection of cells with virus particles.

Viral constructs

cDNAs encoding for CpxII and its mutants (ΔC-CpxII, aa 1–72; ΔN-CpxII, aa 28–134; and CpxII-R63A) were subcloned into the viral plasmid pSFV1 (Invitrogen) upstream of an independent open reading frame that encodes for EGFP. EGFP labeling was used to identify infected cells. Mutant constructs carrying either amino acid deletions or replacements were generated using the overlapping primer method. All mutations were confirmed by DNA sequence analysis (Eurofins MWG Operon). Semliki Forest virus particles were produced as described previously (Ashery et al., 1999). In brief, virus cDNA was transcribed in vitro by using SP6 RNA polymerase (Ambion) after linearization with SpeI. BHK21 cells were transfected by electroporation (400 V and 975 µF) with a combination of 10 µg CpxII and pSFV-helper2 RNA. After 15-h incubation (31°C and 5% CO_2), virions released into the supernatant were collected by low speed centrifugation (200 *g* for 5 min), snap frozen, and stored at −80°C.

Whole-cell capacitance measurements and amperometry

Whole-cell CM measurements and photolysis of caged Ca^{2+} as well as ratiometric measurements of $[Ca^{2+}]_i$ were performed as described previously (Borisovska et al., 2005). The extracellular Ringer's solution contained (mM) 130 NaCl, 4 KCl, 2 $CaCl_2$, 1 $MgCl_2$, 30 glucose, and 10 Hepes-NaOH, pH 7.3. The pipette solution for flash experiments contained (mM) 110 Cs-glutamate, 8 NaCl, 3.5 $CaCl_2$, 5 NP-EGTA, 0.2 fura-2, 0.3 furaptra, 2 MgATP, 0.3 Na_2GTP, 40 Hepes-CsOH, pH 7.3, and 320 mOsm. The flash-evoked capacitance response was approximated with the function $f(x) = A0 + A1(1 - \exp[-t/\tau1]) + A2(1 - \exp[-t/\tau2]) + kt$, in which A0 represents the cell capacitance before the flash. The parameters A1, τ1 and A2, τ2 represent the amplitudes and time constants of the RRP and the SRP, respectively (Rettig and Neher, 2002). Flash-evoked CM responses were scaled after subtraction of the corresponding SR components. The exocytotic delay was defined as the time between the flash and the intersection point of the back-extrapolated fast exponential with the baseline.

Carbon fiber electrode (5-µm diameter; Amoco) manufacturing and amperometric recordings with an amplifier (EPC-7; HEKA) were performed as previously described (Bruns, 2004). For Ca^{2+} infusion experiments, the pipette solution contained (mM) 110 Cs-glutamate, 8 NaCl, 20 diethylene triamine penta-acetic acid, 5 $CaCl_2$, 2 MgATP, 0.3 Na_2GTP, and 40 Hepes-CsOH, pH 7.3 (19 µM of free calcium); 110 Cs-glutamate, 8 NaCl, 20 diethylene triamine penta-acetic acid, 1 $CaCl_2$, 2 MgATP, 0.3 Na_2GTP, and 40 Hepes-CsOH, pH 7.3 (3 µM of free calcium); 140 Cs-glutamate, 8 NaCl, 10 EGTA, 7.5 $CaCl_2$, 2 MgATP, 0.3 Na_2GTP, 20 Hepes-CsOH, and 20 glucose, pH 7.3, (350 nM of free calcium); or 150 Cs-glutamate,

8 NaCl, 10 EGTA, 7.5 $CaCl_2$, 2 MgATP, 0.3 Na_2GTP, 20 Hepes-CsOH, and 40 glucose, pH 7.3 (100 nM of free calcium). Current signals were filtered at 2 kHz, and digitized gap-free signals were filtered at 25 kHz. Amperometric spikes with a charge ranging from 10 to 5,000 fC and peak amplitudes >4 pA were selected for frequency analysis, whereas an amplitude criterion of >7 pA was set for the analysis of single spike characteristics. Given that a single mouse chromaffin granule contributes ∼1 fF CM upon fusion (0.81 ± 0.45 fF/granule, mean ± SD, n = 188; see also Moser and Neher, 1997) and the carbon fiber's detection area (radius of 4 µm; Bruns et al., 2000) covers ∼16% of the chromaffin cell surface (∼300 $µm^2$), the slope of the linear regression (0.172 events/fF) agrees well with the theoretical relationship between both measurements. For fluctuation and rms noise analyses during the prespike signal, only prespike signals with durations longer than 2 ms were considered. For "foot" flicker analysis, the current derivative was again filtered at 1.2 kHz, and fluctuations exceeding the threshold of ±6 pA/ms (∼4× the mean baseline noise) were counted. The number of suprathreshold fluctuations divided by the corresponding foot duration defines the fluctuation frequency.

Immunocytochemistry

Chromaffin cells were processed 3.5 h after virus infection for immunolabeling as described previously (Guzman et al., 2010). In brief, cells were fixed in 4% PFA in PBS for 45 min, washed, and permeabilized with 0.2% Triton X-100 (Sigma-Aldrich). After blocking unspecific binding (2% bovine albumin serum; Sigma-Aldrich), cells were incubated with primary antibodies (1:1,000 rabbit anti-CpxII; Synaptic Systems) overnight and with secondary antibody (1:1,000 Alexa Fluor 543–conjugated goat anti–rabbit; Invitrogen) for 2 h before mounting in glycerol for imaging. Fluorescence images were acquired at room temperature on the stage of a microscope (Axiovert 25; Carl Zeiss) using a 100×, 1.3 NA oil immersion objective (Carl Zeiss) with a charge-coupled device camera (AxioCam MRm; Carl Zeiss) and analyzed with ImageJ software version 1.45 (National Institutes of Health). For quantification, the total intensity of the fluorescent immunolabel was determined within an area of interest comprising the outer cell perimeter.

Secretion analysis in digitonin-permeabilized cells

Before permeabilization, chromaffin cells were washed for 2 min either with 50 or 350 nM of free Ca^{2+} Ringer´s solution, depending on the conditions displayed in Fig. S2. Cells were permeabilized with 10 µM digitonin (EMD Millipore) for 40 s in the presence of 1 mM MgATP/NaGTP. Cells were washed for 20 s using Ringer's solution at the indicated [Ca]i before fixation with 4% PFA (prepared in Ca^{2+}-buffered Ringer's solution; Fig. S2). Immunocytochemistry was performed with a polyclonal rabbit ChrgA antibody purchased from Abcam. Cells were imaged with a microscope (LSM 510; Carl Zeiss) using AxioVision 2008 software (Carl Zeiss) and a 100×, 1.3 NA oil objective at room temperature. Images were analyzed with the software package ImageJ (version 1.45) and SigmaPlot 8.0 (Systat Software, Inc.). To measure the cytoplasmic fluorescence profile of the ChrgA signal, line scans were aligned to the plasma membrane. To determine the overall ChrgA signal within a confocal section, the total fluorescence intensity of the cytoplasm was measured.

Statistical analysis

Values are given as means ± SEM. To determine statistically significant differences, one-way analysis of variance (ANOVA) and a Tukey–Kramer post test for comparing groups were used, if not indicated otherwise.

Online supplemental material

Fig. S1 shows that CpxII clamps tonic secretion in SytI ko cells like in wt cells. Fig. S2 shows that quantification of total fluorescence intensity for ChrgA in the cell cytoplasm confirms the significant loss of granules in CpxII ko cells at 350 nM [Ca]i. Fig. S3 shows that the ΔC and ΔN mutants compete with endogenous CpxII, changing the magnitude and kinetics of synchronized exocytosis. Fig. S4 shows analysis of amperometric spike properties and of expression levels of CpxII wt and mutant proteins. Fig. S5 shows that the SNARE binding mutant CpxII-R63A fails to clamp secretion. Online supplemental material is available at http://www.jcb.org/cgi/content/full/jcb.201311085/DC1.

The authors would like to express their gratitude to Dr. E. Neher for valuable discussions. We are grateful to V. Schmitt and M. Wirth for excellent technical assistance.

The work was supported by grants from the Deutsche Forschungsgemeinschaft (SFB894/A11 to D. Bruns; SFB889/B1 to N. Brose) and by Homburger Forschungsförderungsprogramm (to D. Bruns).

The authors declare no competing financial interests.

Submitted: 20 November 2013
Accepted: 26 February 2014

References

An, S.J., C.P. Grabner, and D. Zenisek. 2010. Real-time visualization of complexin during single exocytic events. *Nat. Neurosci.* 13:577–583. http://dx.doi.org/10.1038/nn.2532

Archer, D.A., M.E. Graham, and R.D. Burgoyne. 2002. Complexin regulates the closure of the fusion pore during regulated vesicle exocytosis. *J. Biol. Chem.* 277:18249–18252. http://dx.doi.org/10.1074/jbc.C200166200

Ashery, U., A. Betz, T. Xu, N. Brose, and J. Rettig. 1999. An efficient method for infection of adrenal chromaffin cells using the Semliki Forest virus gene expression system. *Eur. J. Cell Biol.* 78:525–532. http://dx.doi.org/10.1016/S0171-9335(99)80017-X

Bai, J., C.T. Wang, D.A. Richards, M.B. Jackson, and E.R. Chapman. 2004. Fusion pore dynamics are regulated by synaptotagmin*t-SNARE interactions. *Neuron*. 41:929–942. http://dx.doi.org/10.1016/S0896-6273(04)00117-5

Borisovska, M., Y. Zhao, Y. Tsytsyura, N. Glyvuk, S. Takamori, U. Matti, J. Rettig, T. Südhof, and D. Bruns. 2005. v-SNAREs control exocytosis of vesicles from priming to fusion. *EMBO J.* 24:2114–2126. http://dx.doi.org/10.1038/sj.emboj.7600696

Bracher, A., J. Kadlec, H. Betz, and W. Weissenhorn. 2002. X-ray structure of a neuronal complexin-SNARE complex from squid. *J. Biol. Chem.* 277:26517–26523. http://dx.doi.org/10.1074/jbc.M203460200

Brose, N. 2008. Altered complexin expression in psychiatric and neurological disorders: cause or consequence? *Mol. Cells*. 25:7–19.

Bruns, D. 2004. Detection of transmitter release with carbon fiber electrodes. *Methods*. 33:312–321. http://dx.doi.org/10.1016/j.ymeth.2004.01.004

Bruns, D., and R. Jahn. 1995. Real-time measurement of transmitter release from single synaptic vesicles. *Nature*. 377:62–65. http://dx.doi.org/10.1038/377062a0

Bruns, D., D. Riedel, J. Klingauf, and R. Jahn. 2000. Quantal release of serotonin. *Neuron*. 28:205–220. http://dx.doi.org/10.1016/S0896-6273(00)00097-0

Cai, H., K. Reim, F. Varoqueaux, S. Tapechum, K. Hill, J.B. Sørensen, N. Brose, and R.H. Chow. 2008. Complexin II plays a positive role in Ca2+-triggered exocytosis by facilitating vesicle priming. *Proc. Natl. Acad. Sci. USA*. 105:19538–19543. http://dx.doi.org/10.1073/pnas.0810232105

Cao, P., X. Yang, and T.C. Südhof. 2013. Complexin activates exocytosis of distinct secretory vesicles controlled by different synaptotagmins. *J. Neurosci.* 33:1714–1727. http://dx.doi.org/10.1523/JNEUROSCI.4087-12.2013

Chakrabarti, S., K.S. Kobayashi, R.A. Flavell, C.B. Marks, K. Miyake, D.R. Liston, K.T. Fowler, F.S. Gorelick, and N.W. Andrews. 2003. Impaired membrane resealing and autoimmune myositis in synaptotagmin VII–deficient mice. *J. Cell Biol.* 162:543–549. http://dx.doi.org/10.1083/jcb.200305131

Chapman, E.R. 2008. How does synaptotagmin trigger neurotransmitter release? *Annu. Rev. Biochem.* 77:615–641. http://dx.doi.org/10.1146/annurev.biochem.77.062005.101135

Chen, X., D.R. Tomchick, E. Kovrigin, D. Araç, M. Machius, T.C. Südhof, and J. Rizo. 2002. Three-dimensional structure of the complexin/SNARE complex. *Neuron*. 33:397–409. http://dx.doi.org/10.1016/S0896-6273(02)00583-4

Chicka, M.C., and E.R. Chapman. 2009. Concurrent binding of complexin and synaptotagmin to liposome-embedded SNARE complexes. *Biochemistry*. 48:657–659. http://dx.doi.org/10.1021/bi801962d

Cho, R.W., Y. Song, and J.T. Littleton. 2010. Comparative analysis of *Drosophila* and mammalian complexins as fusion clamps and facilitators of neurotransmitter release. *Mol. Cell. Neurosci.* 45:389–397. http://dx.doi.org/10.1016/j.mcn.2010.07.012

Chow, R.H., L. von Rüden, and E. Neher. 1992. Delay in vesicle fusion revealed by electrochemical monitoring of single secretory events in adrenal chromaffin cells. *Nature*. 356:60–63. http://dx.doi.org/10.1038/356060a0

Fernández-Chacón, R., and G. Alvarez de Toledo. 1995. Cytosolic calcium facilitates release of secretory products after exocytotic vesicle fusion. *FEBS Lett.* 363:221–225. http://dx.doi.org/10.1016/0014-5793(95)00319-5

Fulop, T., S. Radabaugh, and C. Smith. 2005. Activity-dependent differential transmitter release in mouse adrenal chromaffin cells. *J. Neurosci.* 25:7324–7332. http://dx.doi.org/10.1523/JNEUROSCI.2042-05.2005

Geppert, M., Y. Goda, R.E. Hammer, C. Li, T.W. Rosahl, C.F. Stevens, and T.C. Südhof. 1994. Synaptotagmin I: a major Ca2+ sensor for transmitter release at a central synapse. *Cell*. 79:717–727. http://dx.doi.org/10.1016/0092-8674(94)90556-8

Giraudo, C.G., W.S. Eng, T.J. Melia, and J.E. Rothman. 2006. A clamping mechanism involved in SNARE-dependent exocytosis. *Science*. 313:676–680. http://dx.doi.org/10.1126/science.1129450

Giraudo, C.G., A. Garcia-Diaz, W.S. Eng, A. Yamamoto, T.J. Melia, and J.E. Rothman. 2008. Distinct domains of complexins bind SNARE complexes and clamp fusion in vitro. *J. Biol. Chem.* 283:21211–21219. http://dx.doi.org/10.1074/jbc.M803478200

Giraudo, C.G., A. Garcia-Diaz, W.S. Eng, Y. Chen, W.A. Hendrickson, T.J. Melia, and J.E. Rothman. 2009. Alternative zippering as an on-off switch for SNARE-mediated fusion. *Science*. 323:512–516. http://dx.doi.org/10.1126/science.1166500

Groffen, A.J., S. Martens, R. Díez Arazola, L.N. Cornelisse, N. Lozovaya, A.P. de Jong, N.A. Goriounova, R.L. Habets, Y. Takai, J.G. Borst, et al. 2010. Doc2b is a high-affinity Ca2+ sensor for spontaneous neurotransmitter release. *Science*. 327:1614–1618. http://dx.doi.org/10.1126/science.1183765

Guzman, R.E., Y.N. Schwarz, J. Rettig, and D. Bruns. 2010. SNARE force synchronizes synaptic vesicle fusion and controls the kinetics of quantal synaptic transmission. *J. Neurosci.* 30:10272–10281. http://dx.doi.org/10.1523/JNEUROSCI.1551-10.2010

Hobson, R.J., Q. Liu, S. Watanabe, and E.M. Jorgensen. 2011. Complexin maintains vesicles in the primed state in *C. elegans*. *Curr. Biol.* 21:106–113. http://dx.doi.org/10.1016/j.cub.2010.12.015

Huntwork, S., and J.T. Littleton. 2007. A complexin fusion clamp regulates spontaneous neurotransmitter release and synaptic growth. *Nat. Neurosci.* 10:1235–1237. http://dx.doi.org/10.1038/nn1980

Jorquera, R.A., S. Huntwork-Rodriguez, Y. Akbergenova, R.W. Cho, and J.T. Littleton. 2012. Complexin controls spontaneous and evoked neurotransmitter release by regulating the timing and properties of synaptotagmin activity. *J. Neurosci.* 32:18234–18245. http://dx.doi.org/10.1523/JNEUROSCI.3212-12.2012

Kaeser-Woo, Y.J., X. Yang, and T.C. Südhof. 2012. C-terminal complexin sequence is selectively required for clamping and priming but not for Ca2+ triggering of synaptic exocytosis. *J. Neurosci.* 32:2877–2885. http://dx.doi.org/10.1523/JNEUROSCI.3360-11.2012

Kesavan, J., M. Borisovska, and D. Bruns. 2007. v-SNARE actions during Ca(2+)-triggered exocytosis. *Cell*. 131:351–363. http://dx.doi.org/10.1016/j.cell.2007.09.025

Krishnakumar, S.S., D.T. Radoff, D. Kümmel, C.G. Giraudo, F. Li, L. Khandan, S.W. Baguley, J. Coleman, K.M. Reinisch, F. Pincet, and J.E. Rothman. 2011. A conformational switch in complexin is required for synaptotagmin to trigger synaptic fusion. *Nat. Struct. Mol. Biol.* 18:934–940. http://dx.doi.org/10.1038/nsmb.2103

Kümmel, D., S.S. Krishnakumar, D.T. Radoff, F. Li, C.G. Giraudo, F. Pincet, J.E. Rothman, and K.M. Reinisch. 2011. Complexin cross-links prefusion SNAREs into a zigzag array. *Nat. Struct. Mol. Biol.* 18:927–933. http://dx.doi.org/10.1038/nsmb.2101

Lang, T., I. Wacker, I. Wunderlich, A. Rohrbach, G. Giese, T. Soldati, and W. Almers. 2000. Role of actin cortex in the subplasmalemmal transport of secretory granules in PC-12 cells. *Biophys. J.* 78:2863–2877. http://dx.doi.org/10.1016/S0006-3495(00)76828-7

Lin, M.Y., J.G. Rohan, H. Cai, K. Reim, C.P. Ko, and R.H. Chow. 2013. Complexin facilitates exocytosis and synchronizes vesicle release in two secretory model systems. *J. Physiol.* 591:2463–2473.

Lynch, K.L., R.R. Gerona, D.M. Kielar, S. Martens, H.T. McMahon, and T.F. Martin. 2008. Synaptotagmin-1 utilizes membrane bending and SNARE binding to drive fusion pore expansion. *Mol. Biol. Cell*. 19:5093–5103. http://dx.doi.org/10.1091/mbc.E08-03-0235

Malsam, J., F. Seiler, Y. Schollmeier, P. Rusu, J.M. Krause, and T.H. Söllner. 2009. The carboxy-terminal domain of complexin I stimulates liposome fusion. *Proc. Natl. Acad. Sci. USA*. 106:2001–2006. http://dx.doi.org/10.1073/pnas.0812813106

Martin, J.A., Z. Hu, K.M. Fenz, J. Fernandez, and J.S. Dittman. 2011. Complexin has opposite effects on two modes of synaptic vesicle fusion. *Curr. Biol.* 21:97–105. http://dx.doi.org/10.1016/j.cub.2010.12.014

Maximov, A., J. Tang, X. Yang, Z.P. Pang, and T.C. Südhof. 2009. Complexin controls the force transfer from SNARE complexes to membranes in fusion. *Science*. 323:516–521. http://dx.doi.org/10.1126/science.1166505

McMahon, H.T., M. Missler, C. Li, and T.C. Südhof. 1995. Complexins: cytosolic proteins that regulate SNAP receptor function. *Cell*. 83:111–119. http://dx.doi.org/10.1016/0092-8674(95)90239-2

Moser, T., and E. Neher. 1997. Estimation of mean exocytic vesicle capacitance in mouse adrenal chromaffin cells. *Proc. Natl. Acad. Sci. USA*. 94:6735–6740. http://dx.doi.org/10.1073/pnas.94.13.6735

Nagy, G., J.H. Kim, Z.P. Pang, U. Matti, J. Rettig, T.C. Südhof, and J.B. Sørensen. 2006. Different effects on fast exocytosis induced by synaptotagmin 1 and 2 isoforms and abundance but not by phosphorylation. *J. Neurosci.* 26:632–643. http://dx.doi.org/10.1523/JNEUROSCI.2589-05.2006

Neher, E. 2010. Complexin: does it deserve its name? *Neuron*. 68:803–806. http://dx.doi.org/10.1016/j.neuron.2010.11.038

Nickel, W., T. Weber, J.A. McNew, F. Parlati, T.H. Söllner, and J.E. Rothman. 1999. Content mixing and membrane integrity during membrane fusion driven by pairing of isolated v-SNAREs and t-SNAREs. *Proc. Natl. Acad. Sci. USA*. 96:12571–12576. http://dx.doi.org/10.1073/pnas.96.22.12571

Pinheiro, P.S., H. de Wit, A.M. Walter, A.J. Groffen, M. Verhage, and J.B. Sørensen. 2013. Doc2b synchronizes secretion from chromaffin cells by stimulating fast and inhibiting sustained release. *J. Neurosci.* 33:16459–16470. http://dx.doi.org/10.1523/JNEUROSCI.2656-13.2013

Reim, K., M. Mansour, F. Varoqueaux, H.T. McMahon, T.C. Südhof, N. Brose, and C. Rosenmund. 2001. Complexins regulate a late step in Ca2+-dependent neurotransmitter release. *Cell*. 104:71–81. http://dx.doi.org/10.1016/S0092-8674(01)00192-1

Rettig, J., and E. Neher. 2002. Emerging roles of presynaptic proteins in Ca++-triggered exocytosis. *Science*. 298:781–785. http://dx.doi.org/10.1126/science.1075375

Schaub, J.R., X. Lu, B. Doneske, Y.K. Shin, and J.A. McNew. 2006. Hemifusion arrest by complexin is relieved by Ca2+-synaptotagmin I. *Nat. Struct. Mol. Biol.* 13:748–750. http://dx.doi.org/10.1038/nsmb1124

Schonn, J.S., A. Maximov, Y. Lao, T.C. Südhof, and J.B. Sørensen. 2008. Synaptotagmin-1 and -7 are functionally overlapping Ca2+ sensors for exocytosis in adrenal chromaffin cells. *Proc. Natl. Acad. Sci. USA*. 105:3998–4003. http://dx.doi.org/10.1073/pnas.0712373105

Segovia, M., E. Alés, M.A. Montes, I. Bonifas, I. Jemal, M. Lindau, A. Maximov, T.C. Südhof, and G. Alvarez de Toledo. 2010. Push-and-pull regulation of the fusion pore by synaptotagmin-7. *Proc. Natl. Acad. Sci. USA*. 107:19032–19037. http://dx.doi.org/10.1073/pnas.1014070107

Seiler, F., J. Malsam, J.M. Krause, and T.H. Söllner. 2009. A role of complexin-lipid interactions in membrane fusion. *FEBS Lett.* 583:2343–2348. http://dx.doi.org/10.1016/j.febslet.2009.06.025

Sørensen, J.B. 2004. Formation, stabilisation and fusion of the readily releasable pool of secretory vesicles. *Pflügers Arch.* 448:347–362. http://dx.doi.org/10.1007/s00424-004-1247-8

Sørensen, J.B., R. Fernández-Chacón, T.C. Südhof, and E. Neher. 2003. Examining synaptotagmin 1 function in dense core vesicle exocytosis under direct control of Ca2+. *J. Gen. Physiol.* 122:265–276. http://dx.doi.org/10.1085/jgp.200308855

Sørensen, J.B., K. Wiederhold, E.M. Müller, I. Milosevic, G. Nagy, B.L. de Groot, H. Grubmüller, and D. Fasshauer. 2006. Sequential N- to C-terminal SNARE complex assembly drives priming and fusion of secretory vesicles. *EMBO J.* 25:955–966. http://dx.doi.org/10.1038/sj.emboj.7601003

Strenzke, N., S. Chanda, C. Kopp-Scheinpflug, D. Khimich, K. Reim, A.V. Bulankina, A. Neef, F. Wolf, N. Brose, M.A. Xu-Friedman, and T. Moser. 2009. Complexin-I is required for high-fidelity transmission at the endbulb of Held auditory synapse. *J. Neurosci.* 29:7991–8004. http://dx.doi.org/10.1523/JNEUROSCI.0632-09.2009

Tang, J., A. Maximov, O.H. Shin, H. Dai, J. Rizo, and T.C. Südhof. 2006. A complexin/synaptotagmin 1 switch controls fast synaptic vesicle exocytosis. *Cell*. 126:1175–1187. http://dx.doi.org/10.1016/j.cell.2006.08.030

Tokumaru, H., C. Shimizu-Okabe, and T. Abe. 2008. Direct interaction of SNARE complex binding protein synaphin/complexin with calcium sensor synaptotagmin 1. *Brain Cell Biol.* 36:173–189. http://dx.doi.org/10.1007/s11068-008-9032-9

Trifaró, J.M., and M.L. Vitale. 1993. Cytoskeleton dynamics during neurotransmitter release. *Trends Neurosci.* 16:466–472. http://dx.doi.org/10.1016/0166-2236(93)90079-2

Verhage, M., K.J. de Vries, H. Røshol, J.P. Burbach, W.H. Gispen, and T.C. Südhof. 1997. DOC2 proteins in rat brain: complementary distribution and proposed function as vesicular adapter proteins in early stages of secretion. *Neuron*. 18:453–461. http://dx.doi.org/10.1016/S0896-6273(00)81245-3

Voets, T., T. Moser, P.E. Lund, R.H. Chow, M. Geppert, T.C. Südhof, and E. Neher. 2001. Intracellular calcium dependence of large dense-core vesicle exocytosis in the absence of synaptotagmin I. *Proc. Natl. Acad. Sci. USA*. 98:11680–11685. http://dx.doi.org/10.1073/pnas.201398798

Wang, C.T., R. Grishanin, C.A. Earles, P.Y. Chang, T.F. Martin, E.R. Chapman, and M.B. Jackson. 2001. Synaptotagmin modulation of fusion pore kinetics in regulated exocytosis of dense-core vesicles. *Science*. 294:1111–1115. http://dx.doi.org/10.1126/science.1064002

Wang, C.T., J.C. Lu, J. Bai, P.Y. Chang, T.F. Martin, E.R. Chapman, and M.B. Jackson. 2003. Different domains of synaptotagmin control the choice between kiss-and-run and full fusion. *Nature*. 424:943–947. http://dx.doi.org/10.1038/nature01857

Wang, C.T., J. Bai, P.Y. Chang, E.R. Chapman, and M.B. Jackson. 2006. Synaptotagmin-Ca2+ triggers two sequential steps in regulated exocytosis in rat PC12 cells: fusion pore opening and fusion pore dilation. *J. Physiol.* 570:295–307.

Wang, P., M.C. Chicka, A. Bhalla, D.A. Richards, and E.R. Chapman. 2005. Synaptotagmin VII is targeted to secretory organelles in PC12 cells, where it functions as a high-affinity calcium sensor. *Mol. Cell. Biol.* 25:8693–8702. http://dx.doi.org/10.1128/MCB.25.19.8693-8702.2005

Weber, T., B.V. Zemelman, J.A. McNew, B. Westermann, M. Gmachl, F. Parlati, T.H. Söllner, and J.E. Rothman. 1998. SNAREpins: minimal machinery for membrane fusion. *Cell*. 92:759–772. http://dx.doi.org/10.1016/S0092-8674(00)81404-X

Wragg, R.T., D. Snead, Y. Dong, T.F. Ramlall, I. Menon, J. Bai, D. Eliezer, and J.S. Dittman. 2013. Synaptic vesicles position complexin to block spontaneous fusion. *Neuron*. 77:323–334. http://dx.doi.org/10.1016/j.neuron.2012.11.005

Xu, J., K.D. Brewer, R. Perez-Castillejos, and J. Rizo. 2013. Subtle interplay between synaptotagmin and complexin binding to the SNARE complex. *J. Mol. Biol.* 425:3461–3475. http://dx.doi.org/10.1016/j.jmb.2013.07.001

Xue, M., K. Reim, X. Chen, H.T. Chao, H. Deng, J. Rizo, N. Brose, and C. Rosenmund. 2007. Distinct domains of complexin I differentially regulate neurotransmitter release. *Nat. Struct. Mol. Biol.* 14:949–958. http://dx.doi.org/10.1038/nsmb1292

Xue, M., A. Stradomska, H. Chen, N. Brose, W. Zhang, C. Rosenmund, and K. Reim. 2008. Complexins facilitate neurotransmitter release at excitatory and inhibitory synapses in mammalian central nervous system. *Proc. Natl. Acad. Sci. USA*. 105:7875–7880. http://dx.doi.org/10.1073/pnas.0803012105

Xue, M., Y.Q. Lin, H. Pan, K. Reim, H. Deng, H.J. Bellen, and C. Rosenmund. 2009. Tilting the balance between facilitatory and inhibitory functions of mammalian and *Drosophila* Complexins orchestrates synaptic vesicle exocytosis. *Neuron*. 64:367–380. http://dx.doi.org/10.1016/j.neuron.2009.09.043

Xue, M., T.K. Craig, J. Xu, H.T. Chao, J. Rizo, and C. Rosenmund. 2010. Binding of the complexin N terminus to the SNARE complex potentiates synaptic-vesicle fusogenicity. *Nat. Struct. Mol. Biol.* 17:568–575. http://dx.doi.org/10.1038/nsmb.1791

Yang, X., Y.J. Kaeser-Woo, Z.P. Pang, W. Xu, and T.C. Südhof. 2010. Complexin clamps asynchronous release by blocking a secondary Ca(2+) sensor via its accessory α helix. *Neuron*. 68:907–920. http://dx.doi.org/10.1016/j.neuron.2010.11.001

Yoon, T.Y., X. Lu, J. Diao, S.M. Lee, T. Ha, and Y.K. Shin. 2008. Complexin and Ca2+ stimulate SNARE-mediated membrane fusion. *Nat. Struct. Mol. Biol.* 15:707–713. http://dx.doi.org/10.1038/nsmb.1446